1521-009X/44/7/1123–1138$25.00
Drug Metabolism and Disposition
http://dx.doi.org/10.1124/dmd.116.069542
Drug Metab Dispos 44:1123–1138, July 2016

Metabolite Kinetics: The Segregated Flow Model for Intestinal and Whole Body Physiologically Based Pharmacokinetic Modeling to Describe Intestinal and Hepatic Glucuronidation of Morphine in Rats In Vivo

Qi Joy Yang, Jianghong Fan,[1] Shu Chen,[2] Lutan Liu, Huadong Sun,[3] and K. Sandy Pang

Department of Pharmaceutical Sciences, Leslie Dan Faculty of Pharmacy, University of Toronto, Toronto, Ontario, Canada

Received January 16, 2016; accepted April 19, 2016

ABSTRACT

We used the intestinal segregated flow model (SFM) versus the traditional model (TM), nested within physiologically based pharmacokinetic (PBPK) models, to describe the biliary and urinary excretion of morphine 3β-glucuronide (MG) after intravenous and intraduodenal dosing of morphine in rats in vivo. The SFM model describes a partial (5%–30%) intestinal blood flow perfusing the transporter- and enzyme-rich enterocyte region, whereas the TM describes 100% flow perfusing the intestine as a whole. For the SFM, drugs entering from the circulation are expected to be metabolized to lesser extents by the intestine due to the segregated flow, reflecting the phenomenon of shunting and route-dependent intestinal metabolism. The poor permeability of MG crossing the liver or intestinal basolateral membranes mandates that most of MG that is excreted into bile is hepatically formed, whereas MG that is excreted into urine originates from both intestine and liver metabolism, since MG is effluxed back to blood. The ratio of MG amounts in urine/bile $\left(\frac{A^{MG}_{urine}}{A^{MG}_{bile}}\right)$ for intraduodenal/intravenous dosing is expected to exceed unity for the SFM but approximates unity for the TM. Compartmental analysis of morphine and MG data, without consideration of the permeability of MG and where MG is formed, suggests the ratio to be 1 and failed to describe the kinetics of MG. The observed intraduodenal/intravenous ratio of $\frac{A^{MG}_{urine,4h}}{A^{MG}_{bile,4h}}$ (2.55 at 4 hours) was better predicted by the SFM-PBPK (2.59 at 4 hours) and not the TM-PBPK (1.0), supporting the view that the SFM is superior for the description of intestinal-liver metabolism of morphine to MG. The SFM-PBPK model predicts an appreciable contribution of the intestine to first pass M metabolism.

Introduction

It has been recognized that, generally, compartmental modeling is unable to quantitatively address the multiplicity of metabolite formation organs and does not account for sequential metabolism/excretion nor permeability barriers of formed metabolites (Pang et al., 2008; Pang, 2009). In contrast, physiologically based pharmacokinetic (PBPK) models address events of sequential elimination and include transmembrane barriers (de Lannoy and Pang, 1986, 1993; Pang, 2003; Pang et al., 2009; Chow and Pang, 2013) and transporters (Sun et al., 2006, 2010). The intestine, richly endowed with enzymes and transporters (van Herwaarden et al., 2007; Zhang et al., 2007, 2009; Liu et al., 2010), strongly affects first-pass metabolism and controls the flow of substrate to the liver (Pang and Chow, 2012). Intestinally formed metabolites may undergo immediate sequential metabolism or excretion (Pang and Gillette, 1979). When the metabolite possesses good permeability or transporter-linked properties, it will cross the liver cell membrane to endure liver metabolism and/or biliary excretion prior to reaching the lung, heart, and general circulation.

Route-dependent metabolism by the intestine is repeatedly being observed (namely, a higher extent of intestinal metabolism exists when a drug is given orally versus the lower extent or virtual absence of intestine metabolism when the drug is given systemically) (Cong et al., 2000; Doherty and Pang, 2000; Fan et al., 2010). This was observed for erythromycin (Lown et al., 1995) and midazolam (Paine et al., 1996) in humans and for enalapril hydrolysis (Pang et al., 1985) and morphine glucuronidation in the rat intestine (Doherty and Pang, 2000). The lesser extent of intestinal metabolism for systemically delivered drugs is explained by the pattern that a fraction and not the entire intestinal blood flow perfuses and recruits enzymes/excretory transporters in the enterocyte region, with the majority of flow perfusing the inactive, serosal region (Cong et al., 2000; Fan et al., 2010). These observations led to the development of the segregated flow model (SFM), describing that only a partial intestinal flow (5%–30%) reaches the enterocyte region to explain the higher oral versus intravenous intestinal metabolism. In contrast, the traditional model (TM) describes no difference, when the entire intestinal flow perfuses the intestinal tissue as a whole (Cong et al., 2000).

In this study, we examined morphine glucuronidation in the rat in vivo after administration of small doses of natural (−)-morphine (M) in saline

This research was supported by the Canadian Institutes of Health Research [(to K.S.P.)] and the Ontario Graduate Scholarship Program [(to Q.J.Y.)].

Q.J.Y. and J.F. are co-first authors.

[1]Current affiliation: Office of Generic Drugs, Food and Drug Administration, Silver Spring, Maryland.

[2]Current affiliation: Apotex Inc., Toronto, Ontario, Canada.

[3]Current affiliation: Bristol Myers Squibb, Princeton, New Jersey.

dx.doi.org/10.1124/dmd.116.069542.

ABBREVIATIONS: AUC, area under the concentration-time curve; CL, clearance; CV, coefficient of variation; ID, intraduodenal; IS, internal standard; LC, liquid chromatography; M, natural (−)-morphine; *m/z*, mass-to-charge ratio; MG, morphine glucuronide; LC/MS, liquid chromatographic mass spectrometry; PBPK, physiologically based pharmacokinetic; SFM, segregated flow model; TM, traditional model.

into the jugular vein for intravenous or duodenal lumen [or intraduodenal (ID)] dosing, with continuous bile collection via a catheter. We studied M, which enters the cell by passive diffusion (Doherty et al., 2006) and is primarily glucuronidated at the 3-position to form morphine 3β-glucuronide (MG) by the rat UDP-glucuronosyltransferase 2 family, polypeptide b1, Ugt2b1, in the rat intestine and liver (Rane et al., 1985). Morphine is also known to be metabolized by cytochrome P450 (Projean et al., 2003) and undergoes excretion via P-glycoprotein (Böerner 1975; Iwamoto and Klaassen, 1977; Letrent et al., 1999; Wandel et al., 2002) to minor extents. The rat kidney actively secretes but does not metabolize M (Van Crugten et al., 1991; Shanahan et al., 1997). MG is excreted from formation tissues; enterohepatic circulation in rats has been noted (Dahlström and Paalzow, 1978; Horton and Pollack, 1991) but not for the rat with an open bile fistula. The influx permeability clearance of MG through the liver (0.1 $ml \cdot min^{-1} \cdot g^{-1}$ liver) was estimated to be 5%–10% of the flow rate, suggesting the existence of a diffusional barrier for MG to enter the hepatocyte (Doherty et al., 2006). Intestinally formed MG undergoes luminal secretion via the multiple drug resistance-associated protein 2 (Mrp2) and is effluxed into the circulation via the multiple drug resistance-associated protein 3 (Mrp3), in the rat (van de Wetering et al., 2007). MG formed in the liver is biliarily excreted as well as effluxed out. These MG species of intestinal and hepatic origins that reenter the circulation are excreted by the kidney, with clearance (CL) values that are similar to the glomerular filtration rate (Van Crugten et al., 1991). Intuitively speaking, the extents of intestine versus liver formation of MG, reflected by their appearance in urine/bile, should remain the same for both intravenous and intraduodenal dosing, when the flow patterns for the delivery of M to the intestine and liver are the same for different routes of drug administration, as with the TM model. By contrast, when M in the systemic circulation is being partially shunted away from the enterocyte for metabolism with intravenous dosing for the SFM model, the urine/bile ratio of MG for intravenous dosing of M is expected to be lower than that for intraduodenal dosing. The different extents of excretion of MG in bile versus urine for intraduodenal versus intravenous dosing of M could be used to appraise which intestine model, TM or SFM, best describes first-pass metabolism when nested within PBPK models.

Materials and Methods

Materials

M and MG were provided by the National Institutes of Health National Institute on Drug Abuse (Rockville, MD); caffeine, the internal standard (IS), was purchased from Sigma-Aldrich Co. (St. Louis, MO). High-performance liquid chromatography (LC)–grade acetonitrile, methanol, and formic acid were obtained from Fisher Scientific Canada (Ottawa, ON, Canada). Male Sprague-Dawley rats (St. Constant, QC, Canada), weighing 305 ± 10 g (aged 8 to 9 weeks), were used throughout the study.

In Vivo Pharmacokinetic Study

Rats were maintained under constant housing and environmental conditions (temperature, lighting, and diet) according to protocols approved by the University of Toronto. Rats were abstained from food but were given 5% (w/v) glucose water overnight before the day of the study. Pentobarbital (65 $mg \cdot kg^{-1}$, given intraperitoneally) was used to induce anesthesia, since ketamine was previously reported to inhibit morphine glucuronidation (Qi et al., 2010). Under anesthesia, the carotid artery was cannulated with PE50 tubing, which was prefilled with heparinized (1000 U/ml) physiologic saline solution for sampling; the contralateral jugular vein was cannulated for the intravenous administration of M (Hirayama et al., 1990). The intraduodenal dose solution was introduced as a bolus needle injection into the proximal duodenum. A midline incision was made for bile duct cannulation with PE50 tubing. The opened neck and abdominal regions for the surgical manipulations were sutured immediately after drug administration. For intravenous administration, M (expressed as morphine base, 14.9±1.6 $\mu mol \cdot kg^{-1}$ in 0.2 ml saline solution) was administered as a bolus into the jugular vein, followed by flushing of the inline contents with saline. For intraduodenal administration, morphine sulfate (expressed as M, 26.6 ± 0.40 $\mu mol \cdot kg^{-1}$ in 0.3 ml saline solution) was injected into the proximal duodenal lumen. The difference in weights of the syringe before and after the injection was taken as the volume of dose injected, and the dose solution was assayed by LC/mass spectrometry. Blood (0.1 ml) was collected via the carotid artery cannula of the same rat at 0, 1, 5, 10, 15, 30, 45, 60, 90, 120, 180, and 240 minutes after dosing for each rat. Bile was collected in toto via the bile duct cannula at 0, 5, 10, 15, 20, 30, 45, 60, 90, 180, and 240 minutes after dosing into prepared 1.5-ml vials. At the end of study (240 minutes), the entire urinary content was collected from the bladder via sampling with a needle/syringe. All samples were kept frozen at −20°C until analysis.

LC/Mass Spectrometry Assay

Protein Precipitation and Solid Phase Extraction. A set of standards of known, added amounts of M and MG in blood was processed in the same manner as the samples. Caffeine (IS; 10 μl of 3 $\mu g \cdot ml^{-1}$) was added to 100 μl blood, followed by protein precipitation with 400 μl of an equimixture of methanol and acetonitrile, which was found to yield the highest recovery of the compounds. After vortex mixing for 60 seconds and centrifugation at 13,000*g* for 10 minutes, the supernatant was transferred into Sep-Pak Vac C_{18} 3-cc cartridges (200 mg; Waters, Milford, MA). Each cartridge was preconditioned with 2 × 1 ml acetonitrile followed by 2 × 1 ml Millipore water (Millipore, Billerica, MA). After loading of sample, 0.5 ml 5% acetonitrile in water was added into the cartridge and the contents in the cartridge were eluted with 2 × 1 ml acetonitrile. The eluent was pooled and dried under N_2 at room temperature. The residue was reconstituted with 200 μl mobile phase [70% water with 0.1% (v/v) formic acid and 30% acetonitrile with 0.1% (v/v) formic acid], and 5 μl reconstituted sample was injected into the LC–MS/MS system.

Calibration curves for the quantification of M and MG in bile and urine samples were constructed under identical conditions. Because of the differential abundances of MG and M in bile, 10 μl bile (for MG assay) and 40 μl bile (for morphine assay) was assayed in separate runs. Samples were spiked with 5 or 10 μl IS solution, then diluted with saline to 100 μl, before mixing with 400 μl methanol and acetonitrile [1:1 (v/v)] for solid phase extraction loading. For urine analysis, 10 μl of the urine sample was spiked with 10 μl IS solution and diluted to 100 μl with saline, then mixed with 400 μl methanol and acetonitrile [1:1 (v/v)] for solid phase extraction loading. These samples were then processed identically to that described for the blood samples.

LC-MS/MS. LC-MS/MS was composed of an Agilent 1200 series liquid chromatograph coupled to an Agilent 6410 triple-quadrupole mass spectrometer with an electrospray source (Agilent Technologies, Santa Clara, CA). A high-performance LC gradient consisting of the mobile phase components of 0.1% formic acid in water (A) and 0.1% formic acid in acetonitrile (B), increasing from 4% to 30% between 5 and 10 minutes, then returning to 4% over the next minute, was developed to separate MG, morphine, and caffeine (IS) at retention times of 2.6, 4.3, and 10.9 minutes, respectively. Transitions from precursor ion to product ion were observed with multiple reaction monitoring, as shown with the respective mass-to-charge ratio (*m/z*): MG (*m/z* 462 → 286), morphine (*m/z* 286.1 → 165), and caffeine (*m/z* 195 → 138). Values for fragments or voltage and collision energy were 160 V and 32 V for MG, 165 V and 40 V for M, and 85 V and 24 V for caffeine, respectively. The area of each peak, obtained by MassHunter workstation software (Agilent Technologies), was normalized to that of the IS. A good correlation that showed linearity ($R^2 > 0.997$) between the added compound/IS area ratio versus the amount of compound in the sample (blood/bile/urine) was observed. The coefficient of variation (CV) was < 14% for all of the concentrations studied. The intraday CV was between 0.4% and 9.2% for M concentrations ranging between 20 and 2470 $ng \cdot ml^{-1}$ and between 0.9% and 12.9% for MG for concentrations ranging between 16 and 2390 $ng \cdot ml^{-1}$. The data showed good linearity for the blood ($R^2 > 0.997$), urine ($R^2 > 0.98$), and bile ($R^2 > 0.98$) calibration curves, and the limit of quantification was 9.75 and 19.5 $ng \cdot ml^{-1}$ for morphine and MG, respectively.

Data Analysis

Noncompartmental/Compartmental Analyses. The total area under the concentration-time curve (AUC) to infinity was estimated as the sum of AUC_{0-t}, obtained with the trapezoidal rule, and AUC_{extrap}, obtained by dividing the blood

concentration of the last sampling point (C_{last}) by β, the terminal slope. The total body (blood) clearance (CL_{tot}) was calculated as $Dose_{IV}/AUC_{\infty,IV}$. The bioavailability (or F_{sys}) was calculated from the dose-normalized $AUC_{\infty,ID}/AUC_{\infty,IV}$ or approximated by the amounts of M excreted into urine at 4 hours after intraduodenal/intravenous dosing. Concentration and amount data were normalized to dose, and data were expressed means ± S.D.

A two-compartment model for M and a one-compartment model for MG were used for compartmental analysis and fitting of M and MG data (Fig. 1). The total elimination rate constant of M arising from the central compartment (k_{10}) comprises the metabolic (k_m), biliary (k_{bile}), and renal (k_{renal}) excretion rate constants and $k_{m,others}$ for other metabolic pathways; k_a, k_{12}, and k_{21} denote the absorption and intercompartmental rate constants, respectively; and V_1 and F_{abs} are the central volume of distribution and fraction of dose absorbed, respectively. The metabolite, MG, with volume of distribution $V\{mi\}$, is excreted into bile and urine, with rate constants $k\{mi\}_{bile}$ and $k\{mi\}_{renal}$, respectively.

PBPK Models. The TM-PBPK and SFM-PBPK models (Fig. 2) were used for optimization of the intravenous and intraduodenal blood, bile and urine data of M and MG. Five tissues were considered: rapidly perfused (RP) tissue, poorly perfused (PP) tissue, and adipose (AD) tissue, liver (L), and intestine (I), which are denoted as subscripts and interconnected by blood flow (Q). For detailed consideration of first-pass metabolism of M, the liver and intestinal tissues were subcompartmentalized as the tissue and tissue blood compartments to better accommodate the permeability barrier of MG. M in intestinal blood (IB) and liver blood (LB) rapidly exchanges with those in tissue with influx ($CL^M_{in,I}$ and $CL^M_{in,L}$, high values) and efflux ($CL^M_{ef,I}$ and $CL^M_{ef,L}$, high values) clearances, respectively. In liver, M forms MG and other metabolites with intrinsic clearances $CL^{M\rightarrow MG}_{int,met,L,}$ *and* $CL^{M\rightarrow others}_{int,met,L,}$, respectively, or it is biliarily excreted ($CL^{M}_{int,sec,L}$). The MG formed in the intestine and liver is either effluxed out with $CL^{MG}_{ef,I}$ and $CL^{MG}_{ef,L}$or secreted into the intestinal lumen and bile canaliculus with secretory intrinsic clearances $CL^{MG}_{int,sec,I}$ and $CL^{MG}_{int,sec,L}$, respectively. MG does not enter the intestine (Doherty and Pang, 2000) but is able to enter the liver, albeit with low permeability (0.1 $ml\cdot min^{-1}\cdot g^{-1}$ liver) (Doherty et al., 2006). The hepatic, influx clearance of MG into the liver ($CL^{MG}_{in,L}$) was hence assigned (0.1 $ml\cdot min^{-1}\cdot g^{-1}$ liver) (Fig. 2). For simplification, the renal excretion of M and MG from the kidney occurs from the central or blood compartment with renal clearances CL^M_R and CL^{MG}_R, respectively. For the SFM, the intestine tissue is further subdivided into the enterocyte (en) and serosal (s) regions and the corresponding blood regions (enB and sB); the enterocyte flow, Q_{en}, perfusing the metabolically active and transporter-rich region is only a small fraction ($f_Q = 0.05$ to 0.3) of the total intestinal flow rate, Q_I or Q_{PV}; the serosal flow, Q_s, is $(1 - f_Q)\ Q_I$ (Fig. 2B) (Cong et al., 2000).

Fitting. Fitting was conducted by ADAPT 5 Systems Analysis Software (BMSR Biomedical Simulations Resource, version 5; University of Southern California, Los Angeles, CA). The population method and the maximum likelihood with the Expectation-Maximization (EM) algorithm were used to fit individual sets of data (intravenous, $n = 4$; intraduodenal, $n = 3$) and the population data set that is based on individual data sets. We employed a two-compartment model for M and a one-compartment model for the metabolite, MG, to fit individual data sets (data for each rat) and all of the data as a whole (Fig. 1). Fitted results furnished estimates of k_a, total elimination (k_{10}), k_m, k_{bile}, k_{renal}, $k_{m,others}$, k_{12}, k_{21}, V_1, and F_{abs}, with rate equations shown in Appendix A.

Then the TM-PBPK and SFM-PBPK models (Fig. 2) were used for fitting, with assigned physiologic volumes and flows that are obtained from literature values and summarized in Table 1. The mass balance equations for the TM-PBPK and SFM-PBPK models appear in Appendix B. The transport clearances for M ($CL^M_{in,I}$, $CL^M_{ef,I}$, $CL^M_{in,L}$, and $CL^M_{ef,L}$) were first assigned as 5× flow to tissue; the tissue to blood partitioning coefficients of M for the rapidly perfused tissue (K_{RP}), poorly perfused tissue (K_{PP}), and adipose tissue (K_{AD}), calculated according to Rodgers and Rowland (2006, 2007), were used as initial estimates (Table 2) and the parameters were optimized by fitting. Similar K_T values for MG were not needed since transport terms were used for the intestine and liver, the few tissues where MG was distributed. The equations, assumptions, and mass balance equations are shown in Appendix B. Only the unbound species was involved in transport and elimination; the unbound fraction in plasma (f_P) was corrected by the blood/plasma concentration ratio (C_B/C_P) to obtain the unbound fraction in blood, f_B. The tissue unbound fraction (f_T) and the intrinsic metabolic or transport clearance were estimated as a combined parameter. All of the intrinsic clearances for metabolism ($CL_{int,met}$) and secretion ($CL_{int,sec}$) for the intestine (I) and liver (L), as well as the rate constants for absorption (k_a), and fraction of dose absorbed in gut lumen (F_{abs}), were obtained by fitting. F_{abs} is the ratio of $k_a/(k_a+k_g)$ where k_g is the luminal degradation rate constant.

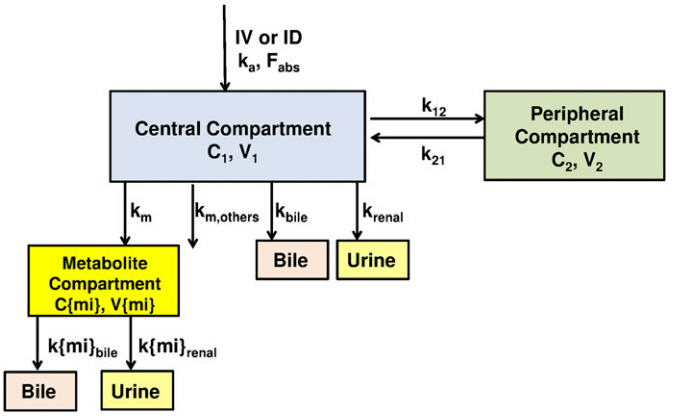

Fig. 1. The two-compartment model scheme for describing the pharmacokinetics of M and MG (or {mi}) (as one compartment); concentrations and amounts have been normalized to dose. k_{renal}, k_{bile}, $k_{m,others}$, and k_m are the first-order rate constants describing M elimination via excretion by the kidney and liver and metabolism to MG formation or other metabolites; $k\{mi\}_{renal}$ and $k\{mi\}_{bile}$ denote the first-order excretion rate constants of MG (or {mi}) by the kidney and liver, respectively. ID, intraduodenal; IV, intravenous.

We also fitted the data with the nested TM- and SFM-PBPK models. With the fitted constants, simulations were extended to time infinity to estimate the amounts of MG in bile and urine for the TM- or SFM-intestine compartment nested in the PBPK model. Ratios of amounts of MG excreted into urine and bile after intraduodenal and intravenous dosing of M were then compared for the TM and SFM-PBPK models. The final model was selected based on the goodness-of-fit criteria, which included convergence, parameter precision, and visual inspection of predicted versus observed values and residual plots. The sum of squared residuals, CV (or standard deviation of fitted parameter/parameter estimate), residual plots, as well as the F test were used to compare goodness of fit of the nested TM- and SFM-PBPK models (Boxenbaum et al., 1974).

Mass Balance Solutions for M and MG Amounts in Bile and Urine. Simple mass balance considerations were developed to illustrate the relationship between the intestine and liver in forming the metabolite in question. It was assumed that the intestine and liver are the only two organs capable of forming MG, and M is completely absorbed. For simplification, MG is assumed as unable to enter the intestine or liver. Mass balance relations involving the intestinal and hepatic availabilities/extraction ratios of M and MG, the formed metabolite, are included to describe the formation of MG by the intestine and liver and in the sequential removal of MG.

Statistical Comparisons

The two-tailed t test was used to compare the means, and a P value of < 0.05 was viewed as significant.

Results

In Vivo Pharmacokinetics of M after Intravenous and Intraduodenal Dosing to Rats: Noncompartmental Analysis

M decayed biexponentially after intravenous dosing, although the biphasic profile was not apparent after intraduodenal dosing (Fig. 3). The terminal half-lives for M, estimated by regression of log-linear portion of decay curves, were identical for intraduodenal and intravenous dosing (61 and 67 minutes; $P > 0.05$). The area under the blood concentration-time curve for M ($AUC_{\infty,IV}$), obtained by summing the AUC by the trapezoidal rule and extrapolated area (C_{last}/β), yielded a total body blood clearance (CL_{tot}) of 6.6 ± 3.3 $ml\cdot min^{-1}$, a value comparable to the blood clearance of 6.31 $ml\cdot min^{-1}$ [$CL_P/(C_B/C_P)$ according to Mistry and Houston (1987), based on plasma clearance, CL_P, of 8.46 and a C_B/C_P ratio of 1.34]. Both M and MG were recovered in bile and urine in different proportions (Fig. 3; Table 3). The renal clearance of M,

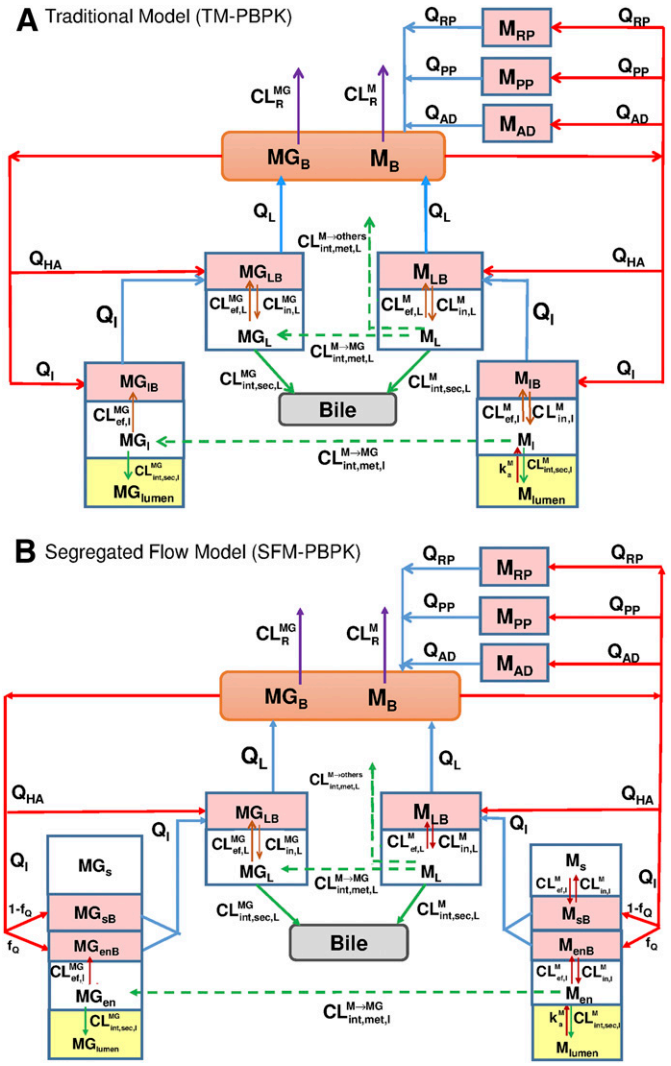

Fig. 2. (A and B) TM-PBPK (A) and SFM-PBPK (B) models for describing the pharmacokinetics of M and MG. MG exhibits poor entry into tissues (including the intestine and liver) and MG is formed in the intestine and liver. Intestinally formed MG enters the liver with influx clearance ($CL_{in,L}^{MG}$) of 1 ml·min^{-1} (according to Doherty et al., 2006), and MG formed in the liver are excreted into bile. See the text for details on the definition of terms.

approximated by $\left(\frac{A_{urine,4h,IV}^{M}}{AUC_{0-4h,IV}^{M}}\right)$, was 2.21 ml·min^{-1}, and the unbound renal clearance was 2.5 ml·min^{-1} after correction for the plasma unbound fraction (f_P = 0.89, Doherty et al., 2006), a value similar to the glomerular filtration rate of 1.01 ml·min^{-1} per 100-g rat, as found with ^{125}I-iothalamat infusion (Marcel de Vries et al., 1997). The bioavailability (F_{sys}) estimated according to the dose-corrected $AUC_{\infty,ID}$/$AUC_{\infty,IV}$ and intraduodenal/intravenous ratio of amounts of morphine recovered in urine at 4 hours were 0.229 and 0.215, respectively (Table 3). These values are lower than that (0.36) from Mistry and Houston (1987) but slightly higher than those reported by Iwamoto and Klaassen (1977) and Dahlström and Paalzow (1978) (0.14 and 0.15, respectively).

MG appeared rapidly in blood, and the terminal half-lives (79 and 72 minutes) of decay of MG from intravenous and intraduodenal dosing of M were slightly but insignificantly longer than those for M ($P > 0.05$, paired t; Table 3). The AUC for MG after intraduodenal dosing of M was two times that of the intravenous dose, showing that use of metabolite AUC^{MG} ratio for intraduodenal/intravenous dosing would not reflect the systemic availability. The renal clearance of MG, approximated by $\frac{A_{urine,4h,IV}^{MG}}{AUC_{4h,IV}^{MG}}$, was 2.63 ml·min^{-1}, and it was 2.68 ml·min^{-1} after correction for the unbound fraction in plasma (0.98); the value is slightly lower than the glomerular filtration rate of Marcel de Vries et al. (1997). The percent dose of MG in bile at 4 hours ($A_{bile,4h}^{MG}$/dose) was 80% higher for intraduodenal dosing than with intravenous dosing, whereas the percent dose of MG recovered in urine at 4 hours ($A_{urine,4h}^{MG}$/Dose)for intraduodenal dosing was 4.65-fold that for the intravenous dose (Table 3). As a result, the $\frac{A_{urine,4h,ID}^{MG}}{A_{bile,4h,ID}^{MG}}$ ratio was 2.55 times that of $\frac{A_{urine,4h,IV}^{MG}}{A_{bile,4h,IV}^{MG}}$ at 4 hours after dosing (Table 3).

Compartmental Modeling of M and MG

Fitting of the blood concentration-time profiles of M and MG after intravenous and intraduodenal dosing was generally satisfactory for both routes of administration (Fig. 3). However, MG in bile was overestimated for intravenous data but underestimated for intraduodenal data, whereas MG in urine was overpredicted for intravenous dosing but underpredicted for intraduodenal dosing. The AUCs provided an estimate of 0.95 for F_{abs} that was higher than observed. The calculated, total clearance ($k_{10}V_1$) was 0.0711 * 140 or 9.95 ml·min^{-1} (Table 4) and was higher than that observed (Table 3). According to the ratio of each rate constant/k_{10}, the pathways for formation of other metabolites (1.4%), biliary excretion (less than 1%), and renal excretion (31%) contributed much less to the total elimination compared with the glucuronidation pathway (67.5%) or k_m/k_{10}.

SFM-PBPK and TM-PBPK Modeling of M and MG

The tissue/blood concentration ratios, or the tissue partitioning ratios were calculated based on the methods of Rodgers and Rowland (2006, 2007) with use of known fractional volumes of the intracellular and extracellular tissue water, neutral lipid and phospholipid, and concentration of binding elements: extracellular albumin, acidic phospholipids, and neutral lipids and phospholipids; the pKa and the oil to water partition coefficient, $P_{o/w}$, for octanol/water and vegetable oil/water were used in the calculation. These were compared with the optimized tissue to blood partitioning coefficients (K_T) that were estimated by fitting (Table 2). Generally, the fitted estimates were within ±2-fold of the calculated values of K_{RP}, K_{PP}, and K_{AD}.

The fits to the PBPK models were much improved compared with that from compartmental fitting (compare Figs. 3 and 4; Table 6). The blood levels of MG were less well predicted by the TM than for the SFM; MG appearance was overestimated in bile both after intravenous and intraduodenal dosing but was underestimated in urine after intraduodenal dosing by TM. Pictorially, predictions by the SFM-PBPK model provided data that closely matched the observed, temporal data for concentration, bile, and urinary profiles up to the 4 hours, compared with the TM (Fig. 4). The fitted parameters of the SFM-PBPK and TM-PBPK are summarized in Table 5. The predicted versus observed data (Figs. 5 and 6) showed that the SFM-PBPK model fitted the data better than the TM-PBPK model. The F test showed that the SFM-PBPK provided the best fits over those for the TM-PBPK and compartmental models (Table 6).

Additional parameters were obtained from PBPK modeling (Table 7). The apparent (unbound) tissue to blood partitioning ratios of M, obtained from the ratio $\frac{f_B^M CL_{in,I}^M}{f_I^M CL_{ef,I}^M}$ and $\frac{f_B^M CL_{in,L}^M}{f_L^M CL_{ef,L}^M}$, are 0.14 to 0.53 for the intestine

TABLE 1

Physiologic volumes and blood flows used for modeling and simulation of rat data

Blood Volume	Value	Blood Flow	Value
	ml		*ml·min^{-1}*
Total blood volume (V_B)[a]	16.2	Hepatic artery (Q_{HA})[g]	3.94
Intestinal blood volume (V_{IB})[b]	1.5	Portal vein (Q_I)[g]	11.7
Serosal blood ($V_{ser,B}$) = f_Q * V_{IB}	—^	[g]	
Enterocyte blood ($V_{en,B}$) = (1 − f_Q) * V_{IB}	—	Rapidly perfused tissue (Q_{HP})[f]	33.3
Intestinal tissue (V_I)[c]	2.2	Poorly perfused tissue (Q_{PP})[f]	20.4
Serosal tissue (V_{ser}) = f_Q * V_I	—	Adipose tissue (Q_{AD})[f]	6.3
Enterocyte tissue (V_{en}) = (1 − f_Q) * V_I	—		
Liver blood (V_{LB})[d]	3.24		
Liver tissue (V_L)[e]	6.59		
Rapidly perfused tissue (heart, kidney, lung, brain) (V_{RP})[f]	15.6		
Poorly perfused tissue (muscle, bone, skin) (V_{PP})[f]	210		
Adipose tissue (V_{AD})[f]	21.2		

^estimated according to value of f_Q, obtained from fitting.
[a]Obtained from Davies and Morris (1993).
[b]Obtained from Peters (2008), based on 40% of intestine volume.
[c]Obtained from Peters (2008), based on 60% of intestine volume.
[d]Obtained from Everett et al. (1956), based on liver weight of 12.1 g, according to Davies and Morris (1993).
[e]Obtained from Gao and Law (2009), based on 60% of organ volume
[f]Obtained from Corley et al. (2005).
[g]Obtained from Gao and Law (2009), based on cardiac output of 89.7 ml·min^{-1} according to Davies and Morris (1993).

and 1.4 to 2.5 for the liver for the TM and SFM-PBPK models. We estimated F_I and F_L as

$$\frac{CL^{M}_{ef,I}}{CL^{M}_{ef,I} + CL^{M}_{int,sec,I}(1 - F_{abs}) + CL^{M\rightarrow MG}_{int,met,I}}$$

and

$$\frac{CL^{M}_{ef,L}}{CL^{M}_{ef,L} + CL^{M\rightarrow MG}_{int,met,L} + CL^{M\rightarrow others}_{int,met,L} + CL^{M}_{int,sec,L}},$$

respectively. We also estimated F_I and F_L according to the equations of Sun and Pang (2010), shown below.

$$\frac{f_Q Q_I CL^{M}_{ef,I}}{f_Q Q_I CL^{M}_{ef,I} + \left(f_Q Q_I + f^{M}_{B} CL^{M}_{in,I}\right)\left[CL^{M\rightarrow MG}_{int,met,I} + CL^{M}_{int,sec,I}(1 - F_{abs})\right]}$$

and

$$\frac{(Q_I + Q_{IIA})(CL^{M}_{ef,L} + CL^{M}_{int,sec,L} + CL^{M\rightarrow MG}_{int,met,L} + CL^{M\rightarrow others}_{int,met,L})}{(Q_I + Q_{IIA})(CL^{M}_{ef,L} + CL^{M}_{int,sec,L} + CL^{M\rightarrow MG}_{int,met,L} + CL^{M\rightarrow others}_{int,met,L}) + f^{M}_{B} CL^{M}_{in,I}(CL^{M}_{int,sec,L} + CL^{M\rightarrow MG}_{int,met,L} + CL^{M\rightarrow others}_{int,met,L})}$$

These F_I values were 0.65 and 0.63 for the TM and 0.46 and 0.28 for the SFM, respectively; the F_L values were 0.57 and 0.71 for the TM and 0.58 and 0.72 for the SFM, respectively (Table 7). The calculated F_I values for the TM and SFM were slightly different with both methods of estimation, with the latter F_I values being influenced by f_Q. The data showed substantial extraction of M by the intestine (E_I of 0.72 to 0.54) according to the TM- and SFM-PBPK models, respectively. By contrast, F_L values were similar regardless of the equation used. For MG that is formed in tissue, the availability or fraction that escapes into the circulation, $F\{mi\}_I$ or $\frac{CL^{MG}_{ef,I}}{CL^{MG}_{ef,I} + CL^{MG}_{int,sec,I}}$, was 0.95 and 0.89 for the intestine, whereas $F\{mi\}_L$ or $\frac{CL^{MG}_{ef,L}}{CL^{MG}_{ef,L} + CL^{MG}_{int,sec,L}}$ was 0.12 to 0.22 for the liver for the TM- and SFM-PBPK models. The data showed little extraction of MG by the intestine but substantial extraction of MG by the liver, according to the TM- and SFM-PBPK models, respectively. The fraction of hepatic clearance of M forming MG, or h_{mi}, was obtained as the ratio of the formation intrinsic clearance/total intrinsic clearance, or > 85% for both the TM- and SFM-PBPK models, showing that glucuronidation is a major elimination pathway in the liver. The fraction of total body clearance of M forming MG, g_{mi}, was around 57%–63%, a value similar to the estimate from the compartmental model. The value is lower since M is excreted unchanged into urine.

The fractional contributions of the intestine and liver to the first-pass removal were estimated. The extents of intestine and liver removal of M are highly dependent on f_Q, the fractional enterocyte flow (Pang and Chow, 2012) (eqs. 1 and 2):

TABLE 2

Initial estimates for tissue partitioning coefficients for morphine and MG and estimated according to the method of Rodgers and Rowland (2006, 2007) for PBPK modeling

Parameter	Morphine		
	Initial Estimate	TM	SFM
Blood unbound fraction (f_B)	0.654[a] 0.634[b]	0.654	0.654
Partition coefficient for rapidly perfused tissue (K_{RP})	3.69[c]	2.05 (47.2)[d]	5.03 (38.8)[d]
Partition coefficient for poorly perfused tissue (K_{PP})	2.37[c]	1.03 (42.8)[d]	1.16 (60.3)[d]
Partition coefficient for adipose tissue (K_{AD})	1.08[c]	0.796 (23.9)[d]	1.63 (20.9)[d]

[a]Method of Doherty et al. (2006), using f_P = 0.89 and C_B/C_P of 1.08 [$f_B = f_P/(C_B/C_P)$].
[b]Method of Mistry and Houston (1987), using f_P = 0.85; C_B/C_P = 1.34.
[c]Calculated according to the method of Rodgers and Rowland (2006, 2007).
[d]Fitted estimates, with percent CV within parentheses.

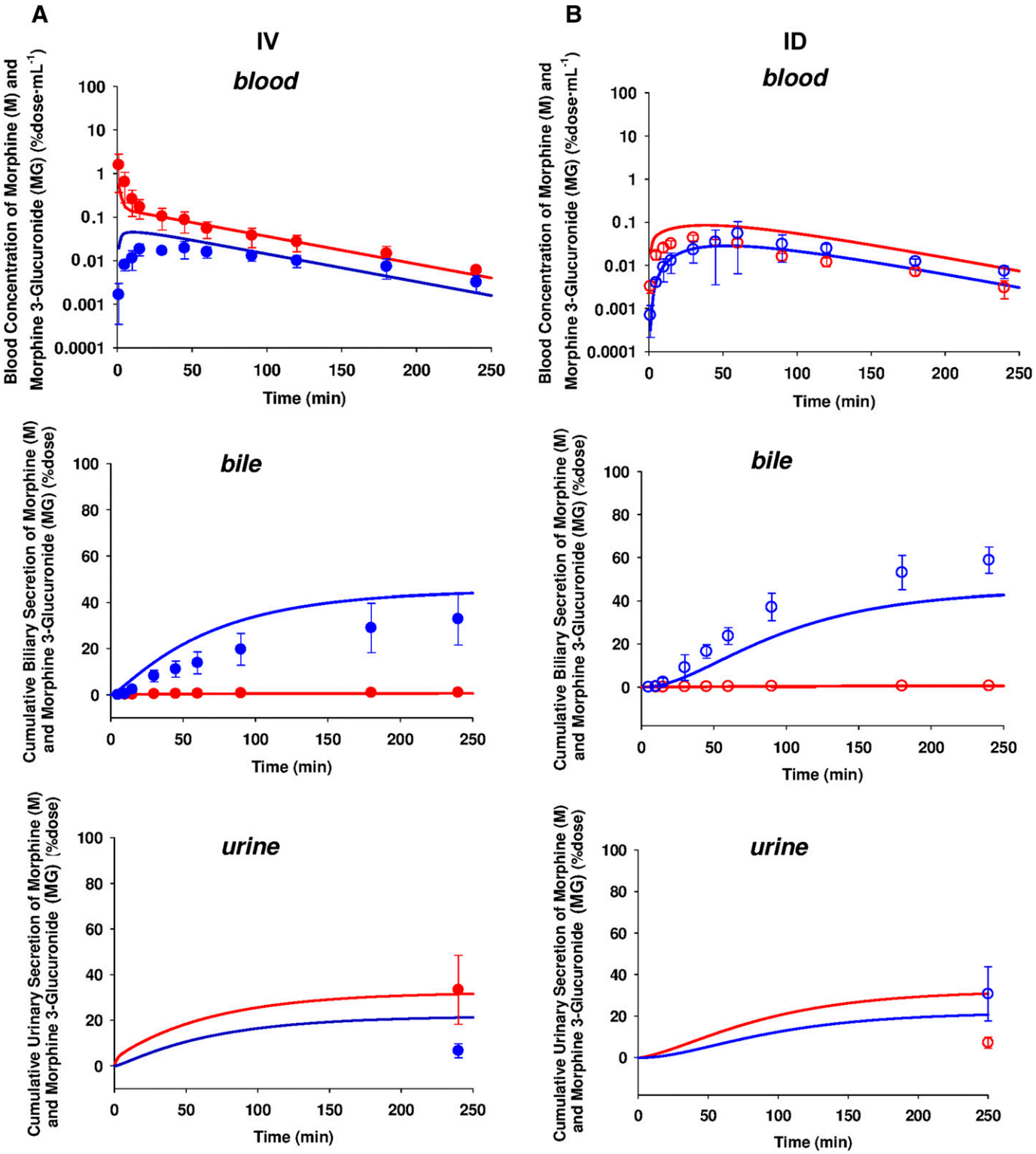

Fig. 3. Observed blood concentration-time profiles of M and MG as well as the cumulative amounts of M and MG in bile and urine after intravenous (A) and intraduodenal dosing (B) of M (IV, solid circles, $n = 4$; ID, open circles, $n = 3$; M and MG are denoted as red and blue symbols, respectively). The fits of the compartmental model (lines) to blood concentrations of M and MG, as well as the cumulative amounts of M and MG in bile and urine after intravenous and intraduodenal administration of M, are shown. Data are presented as means ± S.D. ID, intraduodenal; IV, intravenous.

$$\frac{v_I}{v_I + v_L} = \frac{f_Q Q_I (1 - F_I)}{f_Q Q_I (1 - F_I) + E_L \langle Q_I [f_Q F_I + (1 - f_Q)] + Q_{HA} \rangle} \quad (1)$$

$$\frac{v_L}{v_I + v_L} = \frac{E_L \langle Q_I [f_Q F_I + (1 - f_Q)] + Q_{HA} \rangle}{f_Q Q_I (1 - F_I) + E_L \langle Q_I [f_Q F_I + (1 - f_Q)] + Q_{HA} \rangle} \quad (2)$$

The percent contribution by the intestine was 46%–57% and 9.3%–17% for the TM-PBPK and SFM-PBPK models, respectively; the percent contribution by the liver was 43%–54% and 83%–91% for the TM-PBPK for SFM-PBPK models, respectively (Table 7). These values differed due to the two methods for estimating F_I and F_L. The data

TABLE 3

Noncompartmental data for M and MG for intravenous and intraduodenal data of morphine sulfate administration to the rat (305 ± 16 g)

Values are presented as means ± S.D.

Parameter	Intravenous Dosing (n = 4)	Intraduodenal Dosing (n = 3)	Ratio of Intraduodenal/ Intravenous Dosing	P Value
M				
Dose (μmol·kg^{-1})[a]	14.9 ± 1.6	26.6 ± 0.40	1.79	0.0001*
Rat (g)	299 ± 6	307 ± 12	1.03	0.576
AUC^{M}_{4h} (nM·min·nmol dose^{-1})	183 ± 98	39.9 ± 6.0	0.218	0.057
AUC^{M}_{∞} (nM·min·nmol dose^{-1})	188 ± 97	43.2 ± 6.1	0.229[c]	0.053
$t^{M}_{1/2\beta}$ (min)	61 ± 12	67 ± 23	1.09	0.691
CL_{tot} (ml·min^{-1})	6.57 ± 3.28			
$A^{M}_{bile,4h}$(% dose M excreted into bile at 4h)	0.984 ± 0.508	0.559 ± 0.095	0.568	0.221
$A^{M}_{urine,4h}$ as (% dose M excreted into urine at 4h)	33.4 ± 15.1	7.16 ± 2.68	0.215[d]	0.034*
Percent dose as M excreted into urine and bile (4h)	34.3 ± 15.4	7.71 ± 2.60	0.225	0.034*
CL_R or $A^{M}_{urine,4h}/AUC^{M}_{4h}$ (ml·min^{-1})	2.21 ± 1.24	1.77 ± 0.45	0.800	0.589
MG				
AUC^{MG}_{4h} (nM·min·nmol dose^{-1})	26.2 ± 6.8	53 ± 28	2.02	0.114
AUC^{MG}_{∞} (nM·min·nmol dose^{-1})	30.3 ± 8.2	60.5 ± 29.0	2.0	0.10
$t^{MG}_{1/2\beta}$ (min)	79 ± 11	72 ± 5	0.911	0.82
$A^{MG}_{bile,4h}$ (% dose of MG excreted into bile at 4h)	32.8 ± 11.3	58.8 ± 6.1	1.79	0.016*
$A^{MG}_{urine,4h}$ (% dose MG excreted into urine at 4h)	6.6 ± 3.1	30.7 ± 13.1	4.65	0.015*
CL^{MG}_{R} or $A^{MG}_{urine,4h}/AUC^{MG}_{4h}$ (ml·min^{-1})	2.63 ± 1.19	6.40 ± 3.29	2.43	0.08
Percent dose as MG into urine and bile (4h)	39.5 ± 12.7	89.5 ± 7.0	2.26	0.002*
$A^{MG}_{urine,4h}/A^{MG}_{bile,4h}$	0.212 ± 0.078	0.541 ± 0.274	2.55	0.066
Percent dose – total recovery in bile and urine (4h)[b]	73.8 ± 11	97.2 ± 8.8	1.32	0.030*

[a]Doses of morphine sulfate, as morphine base equivalent.
[b]Summed MG and M amounts in urine and bile.
[c]F_{sys}, based on AUC ratio.
[d]F_{sys}, based on urinary data.
* $P < .05$, unpaired t test

show that the SFM predicts a lesser contribution by the intestine for intestinal-liver removal of M when M in systemic circulation was presented to the intestine. The simulated $\frac{A^{MG}_{urine,4h,ID}}{A^{MG}_{bile,4h,ID}}$, $\frac{A^{MG}_{urine,4h,IV}}{A^{MG}_{bile,4h,IV}}$, and $\frac{A^{MG}_{urine,4h,ID}}{A^{MG}_{bile,4h,ID}} / \frac{A^{MG}_{urine,4h,IV}}{A^{MG}_{bile,4h,IV}}$ for the SFM-PBPK model were closer to the observations than those for the TM-PBPK (Table 8). These values were not changed dramatically upon extrapolation of the data to infinity.

Mass Balance Solutions for TM-PBPK versus SFM-PBPK

We also probed the mass balance relations for the TM versus the SFM. In this examination, several assumptions were made so that meaningful relations could be obtained easily: M is completely absorbed for the intraduodenal dose (F_{abs} = 1) but there is no enterohepatic recirculation for M secreted back to the lumen; M only forms MG and not other metabolites in the intestine and liver. These assumptions are quite reasonable in view of the fitted results (Tables 5 and 7). We further included renal excretion of M, with f_e to define the fraction of the intravenous dose of M excreted unchanged. The most important assumption was that MG in the systemic circulation does not enter the intestine or liver but is renally excreted.

TM-PBPK

According to the TM-PBPK, the serial blood circuit delivering M and MG to the enterocyte (or whole intestine) region and the liver remains unchanged for both intravenous and intraduodenal dosing. The intestine exerts its strategic, anterior placement over the liver in its initial removal of substrates before the species reach the liver. The extent of MG formation by both the intestine and liver is given by (E_I + $F_I E_H$). Thus, the percent contribution to MG formulation during the first pass by the intestine and liver is $\frac{E_I}{E_I + F_I\ E_L}$ and $\frac{F_I\ E_L}{E_I + F_I\ E_L}$, respectively. These fractions, when multiplied by the organ-appropriate available fractions for MG, $F\{mi\}_I$, and $F\{mi\}_L$ for the formed metabolite, yield the extents of formed MG entering the circulation $\left[\frac{E_I F\{mi\}_I}{E_I + F_I\ E_L} + \frac{F_I\ E_L\ F\{mi\}_L}{E_I + F_I\ E_L}\right]$. For the intestine and liver, the portions of the MG formed that are immediately excreted into the gut lumen and bile, respectively, are given by the extraction ratios $E\{mi\}_I$and $E\{mi\}_L$. For intraduodenal and intravenous doses of M ($Dose^{M}_{ID}$ and $Dose^{M}_{IV}$), the amounts of MG in urine and bile for the TM are given by eqs. 3–6:

$$A^{MG,TM}_{urine,ID} = E_I F\{mi\}_I Dose^{M}_{ID} + F_I\ E_L Dose^{M}_{ID} F\{mi\}_L + F_I\ F_L(1-f_e)Dose^{M}_{ID}\left[\frac{E_I F\{mi\}_I}{E_I + F_I\ E_L} + \frac{F_I\ E_L F\{mi\}_L}{E_I + F_I\ E_L}\right] \quad (3)$$

$$A^{MG,\ TM}_{bile,ID} = F_I\ E_L\ Dose^{M}_{ID} E\{mi\}_L + F_I\ F_L\ (1-f_e)Dose^{M}_{ID}\frac{F_I\ E_L\ E\{mi\}_L}{E_I + F_I\ E_L} \quad (4)$$

$$A^{MG,TM}_{urine,IV} = (1-f_e)Dose^{M}_{IV}\frac{(E_I F\{mi\}_I + F_I\ E_L\ F\{mi\}_L)}{E_I + F_I\ E_L} \quad (5)$$

$$A^{MG,TM}_{bile,IV} = (1-f_e)Dose^{M}_{IV}\frac{F_I\ E_L\ E\{mi\}_L}{E_I + F_I\ E_L} \quad (6)$$

The ratios of the amounts of MG in urine/bile for intravenous and intraduodenal dosing of M are identical (eqs. 7–8):

TABLE 4

Fit to two-compartment model for M and MG (mi) after intravenous (14.9 ± 1.6 μmol·kg^{-1}) and intraduodenal (26.6 ± 0.40 μmol·kg^{-1}) doses of morphine sulfate to the rat (305 ± 16 g)

Fitted estimates are percent CV values expressed within parentheses.

Parameter	Definition	Individual Fitted Value	Population Fitted Value
k_{12} (min^{-1})	First-order transfer rate constant between central and peripheral compartments	0.404 (46.9)	0.363 (46.4)
k_{21} (min^{-1})		0.143 (72.9)	0.113 (69.5)
k_{10} (min^{-1})[a]	First-order elimination constant from central compartment	0.0711	0.0735
k_m (min^{-1})	First-order rate constant describing formation of MG from M	0.048 (24.3)	0.047 (20.9)
$k_{m,others}$ (min^{-1})	First-order rate constant describing forming other metabolites from M	0.001 (24.1)	0.001 (25.0)
k_{bile} (min^{-1})	First-order rate constant describing biliary secretion of M	0.0001 (31.0)	0.0004 (31.0)
k_{renal} (min^{-1})	First-order rate constant describing renal excretion of M	0.022 (26.8)	0.021 (23.6)
V_1 (ml)	Volume of distribution of central compartment for M	140 (59.1)	120 (58.0)
k_a (min^{-1})	First-order absorption rate constant of M	0.036 (37.3)	0.034 (35.2)
CL_{tot} (ml·min^{-1})	Total clearance of M	9.95	8.82
$g_{mi} = k_m/k_{10}$	Fraction of total morphine clearance responsible for forming MG	0.675	0.642
F_{abs}	Fraction of dose absorbed	0.94 (30.0)	0.95 (24.8)
$k\{mi\}_{bile}$ (min^{-1})	First-order rate constant describing biliary excretion of MG	0.045 (59.1)	0.040 (46.4)
$k\{mi\}_{renal}$ (min^{-1})[b]	First-order rate constant describing renal excretion of MG	0.020 (12.5)	0.020 (12.1)
$V\{mi\}$ (ml)	Volume of distribution of metabolite compartment	306 (36.0)	292 (29.8)

[a]Calculated based on fitted parameters: $k_{10} = k_m + k_{m,others} + k_{bile} + k_{renal}$.
[b]$k\{mi\} = k\{mi\}_{renal} + k\{mi\}_{bile}$.

$$\frac{A^{MG,TM}_{urine,IV}}{A^{MG,TM}_{bile,IV}} = \frac{E_I F\{mi\}_I}{F_I\ E_L\ E\{mi\}_L} + \frac{F\{mi\}_L}{E\{mi\}_L} \quad (7)$$

$$\frac{A^{MG,TM}_{urine,ID}}{A^{MG,TM}_{bile,ID}} = \frac{E_I F\{mi\}_I}{F_I\ E_L\ E\{mi\}_L} + \frac{F\{mi\}_L}{E\{mi\}_L} = \frac{A^{MG,TM}_{urine,IV}}{A^{MG,TM}_{bile,IV}} \quad (8)$$

In like fashion, it may be shown that $\frac{A^{MG,TM}_{bile,ID}}{A^{MG,TM}_{bile,IV}} = \frac{A^{MG,TM}_{urine,ID}}{A^{MG,TM}_{urine,IV}}$ for the TM-PBPK model.

SFM-PBPK

According to the SFM-PBPK model, MG is formed by the intestine and liver during the first-pass effect, but mostly from the liver upon recirculation due to the segregated flow pattern to the enterocyte region (Cong et al., 2000). With the assumption that circulating levels of M cannot reach the enterocyte region for intestinal metabolism, the amounts of MG detected into urine (A^{MG}_{urine})and bile (A^{MG}_{bile}) according to the SFM for intraduodenal and intravenous dosing of M are given by eqs. 9–12:

$$A^{MG,SFM}_{urine,ID} = E_I F\{mi\}_I Dose^M_{ID} + F_I\ Dose^M_{ID} E_L\ F\{mi\}_L + F_I\ F_L\ (1-f_e) Dose^M_{ID} F\{mi\}_L \quad (9)$$

$$A^{MG,\ SFM}_{bile,ID} = F_I\ E_L\ Dose^M_{ID} E\{mi\}_L + F_I\ F_L\ (1-f_e) Dose^M_{ID} E\{mi\}_L \quad (10)$$

$$A^{MG,SFM}_{urine,IV} = (1-f_e) Dose^M_{IV} F\{mi\}_L \quad (11)$$

$$A^{MG,SFM}_{bile,IV} = (1-f_e) Dose^M_{IV} E\{mi\}_L \quad (12)$$

The ratios of the amounts are as follows (eq. 13 and 14):

$$\frac{A^{MG,\ SFM}_{urine,\ ID}}{A^{MG,\ SFM}_{bile,ID}} = \frac{E_I F\{mi\}_I}{F_I E\{mi\}_L [E_L\ +\ F_L\ (1-f_e)]} + \frac{F\{mi\}_L}{E\{mi\}_L} \quad (13)$$

$$\frac{A^{MG,\ SFM}_{urine,IV}}{A^{MG,\ SFM}_{bile,IV}} = \frac{(1-f_e) Dose^M_{IV} F\{mi\}_L}{(1-f_e) Dose^M_{IV} E\{mi\}_L} = \frac{F\{mi\}_L}{E\{mi\}_L} \quad (14)$$

$\frac{A^{MG,\ SFM}_{urine,ID}}{A^{MG,\ SFM}_{bile,ID}}$ (eq. 13) exceeds $\frac{A^{MG,\ SFM}_{urine,IV}}{A^{MG,\ SFM}_{bile,IV}}$ (eq. 14) by $\frac{E_I F\{mi\}_I}{F_I E\{mi\}_L [E_L + F_L\ (1-f_e)]}$.

Similarly, the ratios of MG amounts in bile and urine after the same doses of intraduodenal and intravenous dosing of M are as follows (eq. 15 and 16):

$$\frac{A^{MG,\ SFM}_{bile,ID}}{A^{MG,\ SFM}_{bile,IV}} = \frac{F_I\ E_L\ Dose^M_{ID} E\{mi\}_L\ +\ F_I\ F_L\ (1-f_e) Dose^M_{ID} E\{mi\}_L}{(1-f_e) Dose^M_{IV} E\{mi\}_L} = \frac{F_I\ E_L + F_I\ F_L\ (1-f_e)}{(1-f_e)} = \frac{F_I\ E_L}{(1-f_e)} + F_I\ F_L \quad (15)$$

$$\frac{A^{MG,\ SFM}_{urine,ID}}{A^{MG,\ SFM}_{urine,IV}} = \frac{E_I F\{mi\}_I Dose^M_{ID} + F_I\ Dose^M_{ID} E_L\ F\{mi\}_L + F_I\ F_L\ (1-f_e) Dose^M_{ID} F\{MG\}_L}{(1-f_e) Dose^M_{IV} F\{mi\}_L} = \frac{E_I F\{mi\}_I}{(1-f_e) F\{mi\}_L} + \frac{F_I\ E_L}{(1-f_e)} +\ F_I\ F_L \quad (16)$$

$\frac{A^{MG,\ SFM}_{urine,ID}}{A^{MG,\ SFM}_{urine,IV}}$ (eq. 16) exceeds $\frac{A^{MG,\ SFM}_{bile,ID}}{A^{MG,\ SFM}_{bile,IV}}$ (eq. 15) by $\frac{E_I F\{mi\}_I}{(1-f_e) F\{mi\}_L}$.

From the above analyses, differences are expected to exist between the TM-PBPK and SFM-PBPK models. The identities $\frac{A^{MG,TM}_{urine,ID}}{A^{MG,TM}_{urine,IV}} = \frac{A^{MG,TM}_{bile,ID}}{A^{MG,TM}_{bile,IV}}$ and $\frac{A^{MG,TM}_{urine,IV}}{A^{MG,TM}_{bile,IV}} = \frac{A^{MG,TM}_{urine,ID}}{A^{MG,TM}_{bile,ID}}$ exist for the TM, and these relations are in stark contrast with those shown for the SFM, where $\frac{A^{MG,SFM}_{urine,ID}}{A^{MG,SFM}_{urine,IV}} > \frac{A^{MG,SFM}_{bile,ID}}{A^{MG,SFM}_{bile,IV}}$ and $\frac{A^{MG,SFM}_{urine,ID}}{A^{MG,SFM}_{bile,ID}} > \frac{A^{MG,SFM}_{urine,IV}}{A^{MG,SFM}_{bile,IV}}$. For cases in which M from the circulation would enter the intestine via $f_Q Q_I$, the true difference would fall in between unity (for the TM) and the theoretical SFM-PBPK estimate from the above example, since MG is able to enter the liver from the circulation and M is shunted away for metabolism by the intestine. These differences are exploited to discriminate between the SFM-PBPK and TM-PBPK models. It is further interesting to note that when there is complete absorption of M and absence of intestinal glucuronidation/secretion (F_I = 1 and E_I = 0), $\frac{A^{MG,\ SFM}_{urine,ID}}{A^{MG,\ SFM}_{bile,ID}} = \frac{A^{MG,\ SFM}_{urine,IV}}{A^{MG,\ SFM}_{bile,IV}} = \frac{F\{MG\}_L}{E\{MG\}_L}$, and $\frac{A^{MG,\ SFM}_{bile,ID}}{A^{MG,\ SFM}_{bile,IV}} = \frac{A^{MG,\ SFM}_{urine,ID}}{A^{MG,\ SFM}_{urine,ID}} = \frac{E_L}{(1-f_e)} + F_L$.

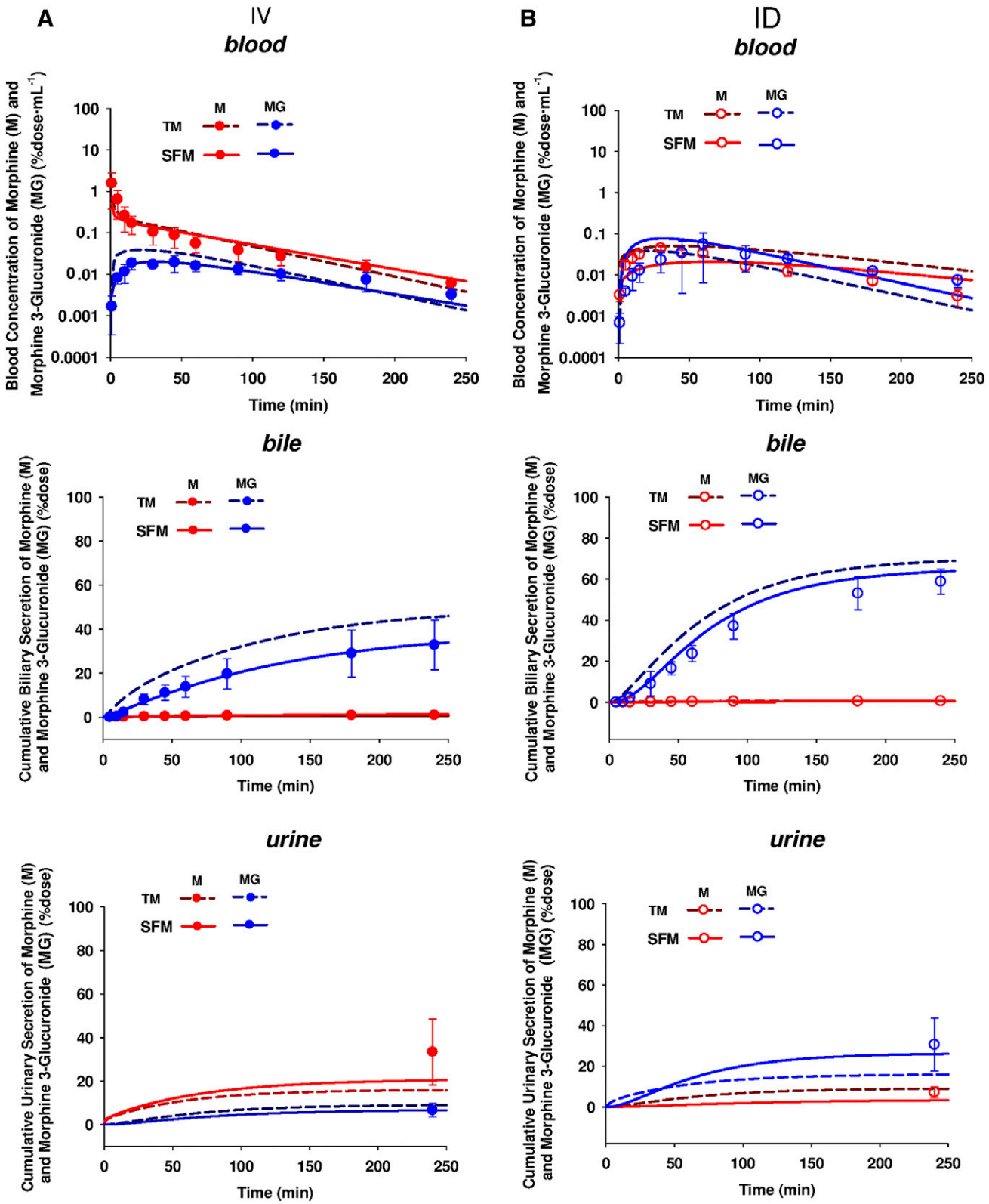

Fig. 4. (A and B) Observed blood concentration-time profiles of M and MG as well as the cumulative amounts of M and MG in bile and urine after intravenous (A) or intraduodenal (B) administration of M (IV, solid circles, $n = 4$; ID, open circles, $n = 3$; M and MG are denoted as red and blue symbols, respectively). Fitting was performed according to the TM or SFM models nested in PBPK models (TM-PBPK or SFM-PBPK). The fits of the model to blood concentrations of M and MG, as well as cumulative amounts of M and MG in bile and urine after intravenous and intraduodenal administration of M (SFM, solid line; TM, dashed line), are shown. Data are presented as means ± S.D. and are the same as those in Fig. 3. Note the improved correlation between predictions and observations for M and MG for the SFM and the less optimal fit of MG with the TM. ID, intraduodenal; IV, intravenous.

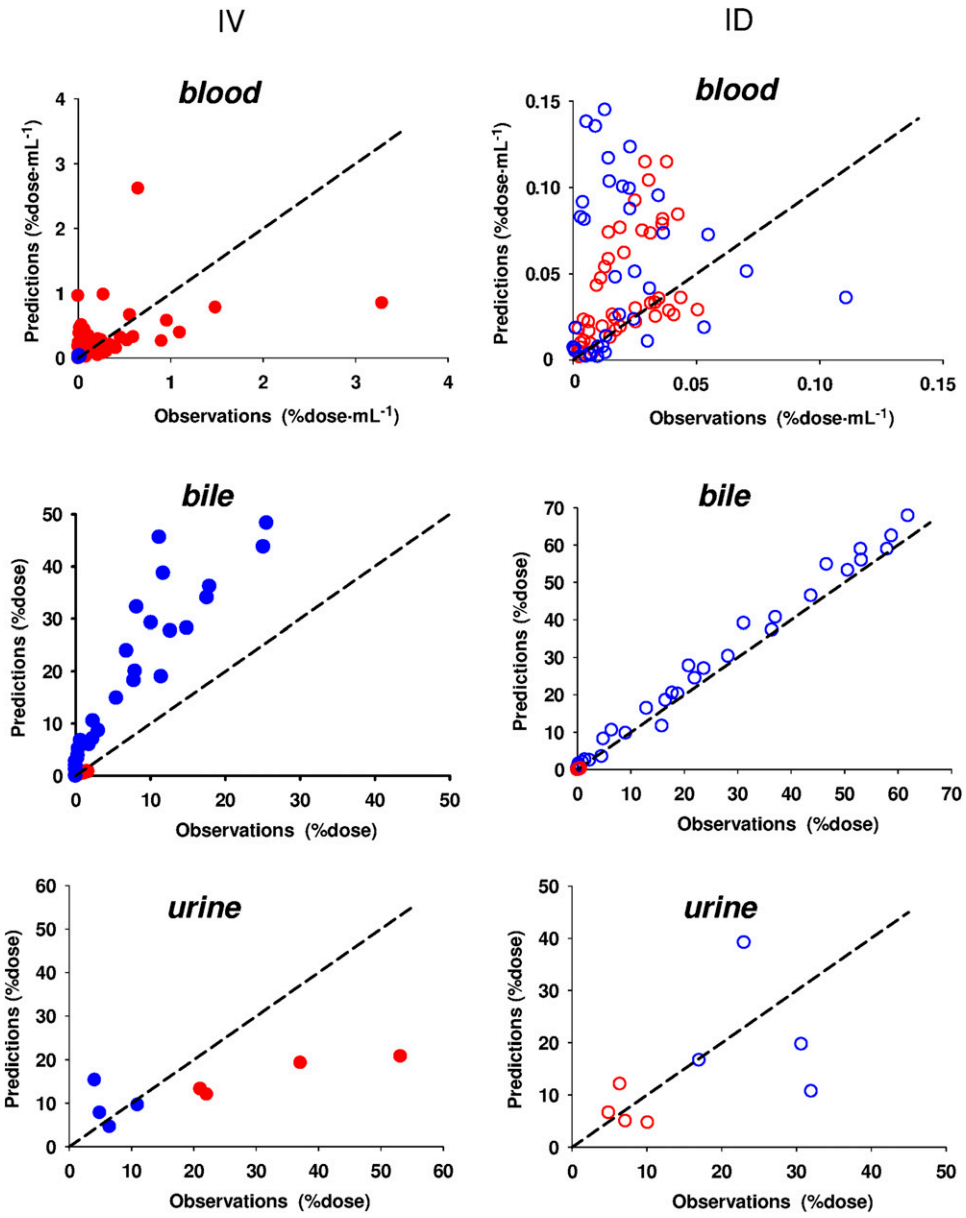

Fig. 5. Plots of observations versus predictions for M (red) and MG (blue) in blood, bile, and urine after intravenous (solid symbols) or intraduodenal (open symbols) administration using the TM-PBPK. The black line denotes the line of identity. ID, intraduodenal; IV, intravenous.

Discussion

With recognition that the intestine can significantly reduce the orally or intraduodenally absorbed dose during first-pass metabolism and that differential induction and inhibition patterns of the enzymes and transporters exist (see Pang and Chow, 2012; Chow and Pang, 2013), much effort is extended to separate the contributions of the intestine and liver in first-pass metabolism. The direct observations on intestinal metabolism could be deciphered for lorcainide metabolism in portacaval shunts in rodents (Gugler et al., 1975; Giacomini et al., 1980; Plänitz, et al., 1985) and midazolam oxidation in anhepatic patients after duodenal and intravenous administrations during transplant surgery (Paine et al., 1996). Others examined specific gene knockdown of Cyp3a and NADPH–cytochrome P450 reductase within the intestinal versus hepatic tissue to directly demonstrate the effect of the knockdown of intestinal versus liver enzymes in first-pass metabolism in vivo (van Herwaarden et al., 2007; Zhang et al., 2007, 2009). The method of comparison of plasma or blood AUCs of drug after oral, intraportal, and intravenous administration, supplemented by in vitro metabolic data, is commonly used to identify the presence of intestinal and extrahepatic versus liver drug metabolism (Iwamoto and Klaassen, 1977; Iwamoto et al., 1982; Cassidy and Houston, 1984, Mistry and Houston, 1987; Liu et al., 2010). Judging merely from the AUC of the blood concentration of the MG or formed metabolite, AUC^{MG}, it becomes difficult to tease out each of the individual contributions of the intestine and liver since multiple tissues are involved in the formation and sequential metabolism of the metabolite (Sun and Pang, 2010). The situation becomes more complex for metabolite kinetics when the metabolite formed undergoes sequential elimination (by metabolism or excretion) (Pang and Gillette, 1979), when a permeability barrier exists (de Lannoy and Pang, 1986), and when the intestine with segregated flow is involved for metabolite formation (Cong et al., 2000). The metabolism of M to MG by the intestine and liver and the immediate excretion of MG in the formation organs exemplify this situation.

The inadequacy of the compartmental model is shown readily. The compartmental approach (Fig. 1) overpredicted MG excretion into bile

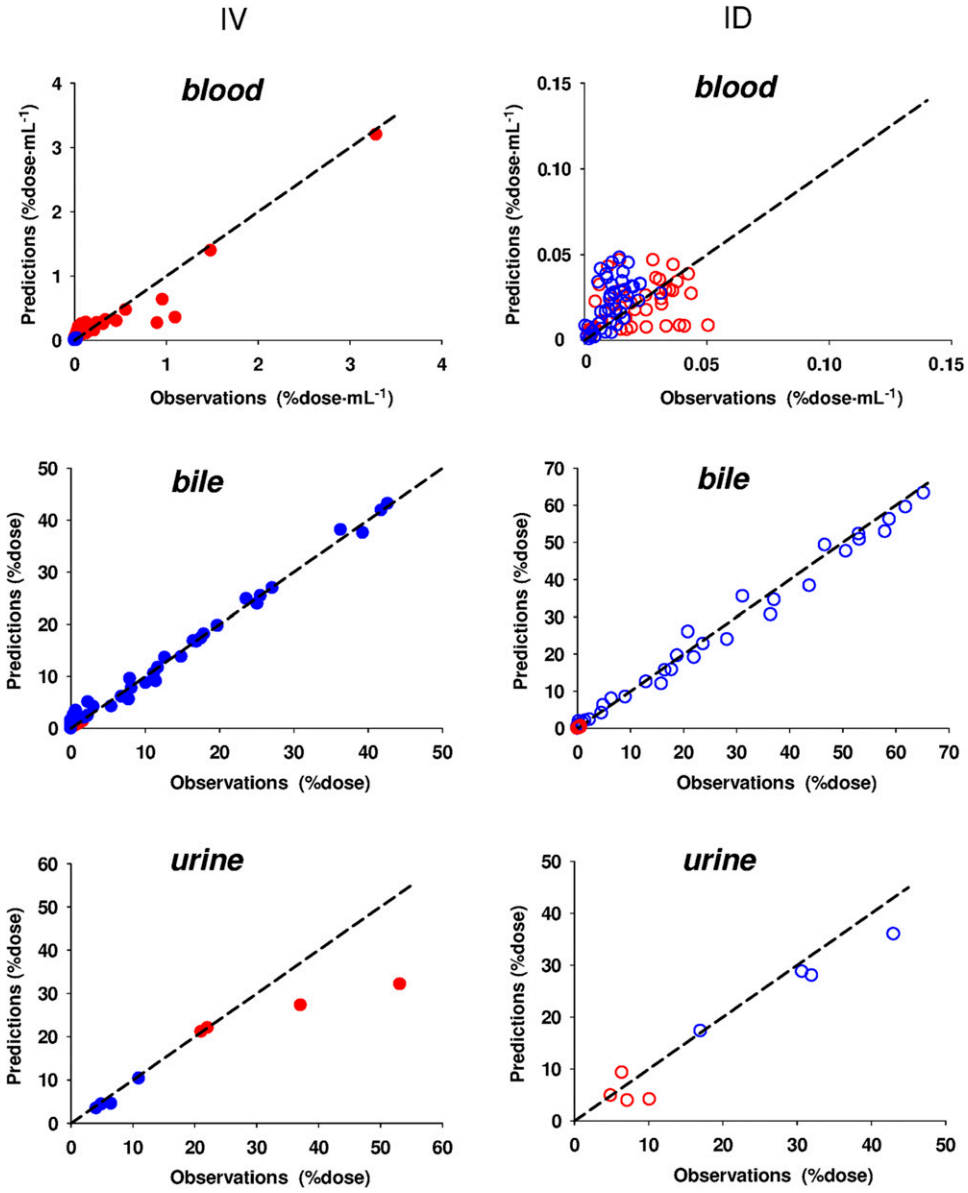

Fig. 6. Plots of observations versus predictions for M (red) and MG (blue) in blood, bile, and urine after intravenous (solid symbols) or intraduodenal (open symbols) administration using the SFM-PBPK. The black line denotes the line of identity. Note that the SFM-PBPK showed here shows a superior correlation between predictions and observations compared with the TM-PBPK (Fig. 5). ID, intraduodenal; IV, intravenous.

for intravenous dosing but underpredicted MG excretion for intraduodenal dosing of M; it also overpredicted MG excretion in urine for intravenous dosing, whereas it underpredicted MG excretion for intraduodenal dosing. The CL_{tot} was 8.8 ml·min^{-1} (Table 4), slightly overpredicting the observed CL_{tot} (6.57 ml·min^{-1}); a higher F_{abs} of approximately 0.95 (Table 4) versus that observed was obtained. Although the comparison of k_m/k_{10} yielded the extent of MG formation (67.5%), other important parameters are unobtainable (compare Table 4 with Tables 5 and 7).

By contrast, we obtain much more insight on M and MG handling with TM- and SFM-PBPK modeling. The final model consists of uptake, transport, and metabolic pathways of M and MG (Table 5), when the liver ($CL_{in,L}^{MG}$as 1 ml·min^{-1}) and intestinal ($CL_{in,I}^{MG}$as 0 ml·min^{-1}) influx clearances for MG were assigned (Fig. 2), and sequential removal of MG is via secretion, in contrast with other metabolites that may undergo further metabolism (Pang and Gillette, 1979). We had tested other PBPK models ($CL_{in,L}^{MG}$= 0 and $CL_{in,I}^{MG} > 0$), but the fit did not improve. The final model revealed information on the effective partitioning ratio into tissue (0.14 and 0.53 for the intestine and 1.4 and 2.5 for the liver based on the TM-PBPK or SFM-PBPK model), and estimates of h_{mi} and g_{mi}, the fractions of hepatic and total body clearance of M forming MG, respectively, with full accounting of the immediate excretion of the nascently formed MG, as $F\{mi\}_I$ and $F\{mi\}_L$ (Table 7). Moreover, the estimates of F_I and F_L that dissect the contribution of the intestine and liver first-pass removal were provided. We emphasize that there are differences in intestinal metabolism when M is entering the intestine from the circulation, and the SFM predicted a smaller intestinal contribution than the TM that during the recirculation of M (Table 7).

In pursuit of whether the SFM is superior to the TM in describing intestinal metabolism of morphine in vivo, we nested these intestinal models into the PBPK model for data fitting (Fig. 2). When both the intestine and liver are involved in formation of the metabolite, we illustrate that the metabolic data are best used to provide discrimination between the SFM-PBPK versus the TM-PBPK model. Therefore, we examined the metabolism of M and excretion of MG. M enters cells freely by passive diffusion, whereas the formed metabolite MG is poorly permeable across the intestine and liver basolateral membranes (Doherty

TABLE 5

Fitted parameters for the PBPK models, with nested TM or SFM intestinal models, showing that SFM is the superior model

Values are presented as means ± CV%.

Fitted Parameter	Definition	TM	SFM
f_Q	Fraction of Q_I to enterocyte region	1	0.10 (11.7)
k_a (min^{-1})	Absorption rate constant of morphine	0.03 (12.6)	0.028 (7.91)
F_{abs}	Fraction of dose absorbed in gut lumen	0.90 (10.2)	0.92 (10.7)
$f_B^M CL_{in,I}$ ($ml \cdot min^{-1}$)	Net influx clearance of morphine in the intestine	0.821 (44.9)	1.38 (49.2)
$f_I^M CL_{ef,I}$ ($ml \cdot min^{-1}$)	Net efflux clearance of M in intestine	5.99 (34.9)	2.60 (39.9)
$f_B^M CL_{in,L}$ ($ml \cdot min^{-1}$)	Net influx clearance of M in liver	15.0 (43.8)	14.5 (17.6)
$f_L^M CL_{ef,L}$ ($ml \cdot min^{-1}$)	Net efflux clearance of M in liver	10.6 (10.0)	5.90 (14.0)
$f_I^M CL_{int,met,I}^{M \rightarrow MG}$ ($ml \cdot min^{-1}$)	Metabolic intrinsic clearance of M forming MG in intestine	3.14 (34.2)	2.93 (22.9)
$f_I^M CL_{int,sec,I}^{M}$ ($ml \cdot min^{-1}$)	Net intestinal intrinsic secretion clearance for M	1.59 (9.92)	2.09 (11.1)
$f_L^M CL_{int,met,L}^{M \rightarrow MG}$ ($ml \cdot min^{-1}$)	Metabolic intrinsic clearance of M forming MG in liver	7.43 (16.5)	3.73 (28.3)
$f_L^M CL_{int,met,L}^{M \rightarrow others}$ ($ml \cdot min^{-1}$)	Metabolic intrinsic clearance of M forming other metabolites in liver	0.35 (12.0)	0.51 (21.4)
$f_L^M CL_{int,sec,L}^{M}$ ($ml \cdot min^{-1}$)	Net biliary clearance of M	0.06 (12.7)	0.13 (18.8)
$f_B^M CL_R^M$ ($ml \cdot min^{-1}$)	Net renal clearance of M	0.91 (54.5)	1.27 (57.8)
CL_R^M ($ml \cdot min^{-1}$)	Renal clearance for M after correcting for f_B^M (Table 2)	1.39	1.94
$f_I^{MG} CL_{ef,I}^{MG}$ ($ml \cdot min^{-1}$)	Efflux clearance for MG in the intestine	4.09 (24.1)	2.97 (4.7)
$f_I^{MG} CL_{int,sec,I}^{MG}$ ($ml \cdot min^{-1}$)	Intestinal intrinsic secretion for MG	0.22 (21.8)	0.35 (11.4)
$f_B^M CL_{in,L}^{MG}$ ($ml \cdot min^{-1}$)	Influx clearance for MG in the liver (assigned)	1	1
$f_L^{MG} CL_{ef,L}^{MG}$ ($ml \cdot min^{-1}$)	Efflux clearance for MG in the liver	0.04 (62.1)	0.2 (56.8)
$f_L^{MG} CL_{int,sec,L}^{MG}$ ($ml \cdot min^{-1}$)	Biliary clearance of MG	0.29 (38.3)	0.70 (43.5)
$f_B^{MG} CL_R^{MG}$ ($ml \cdot min^{-1}$)	Net renal clearance of MG	2.40 (54.5)	0.40 (48.3)
CL_R^{MG} ($ml \cdot min^{-1}$)	Renal clearance for MG after correcting for $f_B^{MG} = 0.98$	2.45	0.41
AIC	Akaike information criteria	317	308

et al., 2006; van de Wetering et al., 2007). MG formed in the intestine and liver is effluxed out by Mrp3 or excreted by Mrp2 into the lumen or bile, respectively. The MG in bile originates mostly from M metabolism in liver since little MG formed from intestine entered the liver, with both MG speceis excreted into bile. In contrast, MG in urine originates from both the intestine and liver. Thus, after making some simple assumptions, differences are expected between the SFM-PBPK and TM-PBPK predictions based on our simple mass balance solutions on the ratio, $A_{urine}^{MG}/A_{bile}^{MG}$ after intraduodenal and intravenous dosing of M. The $A_{urine}^{MG,TM}/A_{bile}^{MG,TM}$ ratio according to the TM remains unchanged for both intraduodenal and intravenous dosing (eq. 8) since, according to this model, the intestine exerts itself as the anterior organ within the intestine-liver unit, regardless of whether morphine is entering via the intraduodenal route or from the systemic circulation. With the extreme assumption that M in circulation is completely shunted away from the intestine and MG does not cross membranes into the intestine or liver, $A_{urine}^{MG,SFM}/A_{bile}^{MG,SFM}$ for SFM after intraduodenal dosing of M would exceed that for intravenous dosing (see eqs. 15 and 16). However, there is some delivery of M to the enterocyte region (namely, f_Q is not zero, but f_Q is approximately 0.1) and $CL_{in,L}^{MG} = 1\ ml \cdot min^{-1}$. Clearly, the predictions for the SFM would fall between this extreme condition for the SFM and that for the TM. Indeed, we observed that $\frac{A_{urine,ID}^{MG}}{A_{bile,ID}^{MG}}$ (0.541) $> \frac{A_{urine,IV}^{MG}}{A_{bile,IV}^{MG}}$ (0.212), and the ratio for $A_{urine}^{MG}/A_{bile}^{MG}$ after intraduodenal dosing of M was 2.55 times that after intravenous dosing (Table 3). These observations agree well with the predicted SFM ratio, being >1 (eq. 16), whereas for TM (eq. 8), the ratio equals 1 (Table 8). Moreover, the superior fit to the SFM model (Figs. 5 and 6; Table 6), and the simulated patterns for M and MG correlated better with the observed data than TM (Figs. 4–6), suggesting that the SFM-PBPK describes first-pass removal of M and MG in rats in vivo much better than the TM-PBPK. With these observations, we may conclude that systemically delivered morphine is partially shunted away from reaching the enterocyte region containing Ugt2b1 for glucuronidation.

The question that remains is why there is urgency to identify the proper intestinal model in PBPK modeling. Recent examination of intestinal flow models emphasized that the type of intestinal flow model chosen is important: TM, Q_{Gut} model (Yang et al., 2007), or SFM, in which the fractional flow to enterocyte region (f_Q) is 1, 0.484, and 0.1–0.3, respectively (Pang and Chow, 2012). For most substrates, the fitted f_Q is < 0.2 (Pang and Chow, 2012; Chow and Pang, 2013), and it is 0.10 for this study (Table 5). Since the percent contribution of the intestine during recirculation of M is dependent on f_Q (see equations shown as footnotes to Table 7), we expect the ranking of SFM < Q_{Gut} model < TM to stand, whereas the opposite exists for the percent contribution of liver (SFM > Q_{Gut} model > TM) (Pang and Chow, 2012). These interpretations could affect the translation of in vitro microsomal activity to the metabolic intrinsic clearance, $CL_{int,met}$, in vivo. The intestinal flow model chosen to represent the enterocyte flow may also influence values of F_I and E_I. The data of Mistry and Houston (1987) revealed a 24-fold microsomal activity ratio ($CL_{int,met,L}/CL_{int,met,I}$) in vitro; yet in vivo E_I and E_L values of 0.33 and 0.47, respectively, correlated with only a 37-fold intrinsic clearance ratio (calculated $CL_{int,met,L}/CL_{int,met,I}$) in vivo for morphine glucuronidation in the rat. Therefore, the flow pattern to the enterocyte region of the intestine may play a role in altering in vitro–in vivo extrapolation.

TABLE 6

Comparison of the goodness of fit among the three models

Statistic Parameters	Two-Compartmental Model	TM-PBPK	SFM-PBPK
Weighted residual sum of squares	445	419	394
F value			
Versus two-compartment model	—^	4.31[a]	7.83[a]
Versus TM-PBPK model	—	—	23.0[a]

^not applicable;

[a]Calculated F score > critical F value of 4.0, suggesting the order of goodness of fit: two-compartment model < TM-PBPK < SFM-PBPK.

TABLE 7

Additional parameters obtained from estimates in Table 5

Parameter	Definition	TM-PBPK	SFM-PBPK
$\frac{f_B^M CL_{in,I}^M}{f_I^M CL_{ef,I}^M}$	Ratio of effective uptake/efflux clearance of M in intestine, or intestine to blood partitioning of unbound morphine	0.137	0.531
$\frac{f_B^M CL_{in,L}^M}{f_L^M CL_{ef,L}^M}$	Ratio of effective uptake/efflux clearance of M in liver, or liver to blood partitioning ratio of unbound morphine	1.42	2.46
F_I	Intestinal availability of M		
	$\frac{CL_{ef,I}^M}{CL_{ef,I}^M + CL_{int,sec,I}^M(1-F_{abs}) + CL_{int,met,I}^{M\to MG}}$	0.654	0.457
	$\frac{f_Q Q_I CL_{ef,I}^M}{f_Q Q_I CL_{ef,I}^M + (f_Q Q_I + f_B^M CL_{in,I}^M)\left[CL_{int,met,I}^{M\to MG} + CL_{int,sec,I}^M(1-F_{abs})\right]}$[d]	0.629	0.282
F_L	Hepatic availability of M		
	$\frac{CL_{ef,L}^M}{CL_{ef,L}^M + CL_{int,met,L}^{M\to MG} + CL_{int,met,L}^{M\to others} + CL_{int,sec,L}^M}$	0.574	0.574
	$\frac{(Q_I + Q_{HA})(CL_{ef,L}^M + CL_{int,sec,L}^M + CL_{int,met,L}^{M\to MG} + CL_{int,met,L}^{M\to others})}{(Q_I + Q_{HA})(CL_{ef,L}^M + CL_{int,sec,L}^M + CL_{int,met,L}^{M\to MG} + CL_{int,met,L}^{M\to others}) + f_B^M CL_{in,L}^M (CL_{int,sec,L}^M + CL_{int,met,L}^{M\to MG} + CL_{int,met,L}^{M\to others})}$[d]	0.710	0.717
$F_{sys} = F_{abs} * F_I * F_L$	Systemic bioavailability:		
	$F_{abs} * \frac{CL_{ef,I}^M}{CL_{ef,I}^M + CL_{int,sec,I}^M(1-F_{abs}) + CL_{int,met,I}^{M\to MG}} * \frac{CL_{ef,L}^M}{CL_{ef,L}^M + CL_{int,met,L}^{M\to MG} + CL_{int,met,L}^{M\to others} + CL_{int,sec,L}^M}$	0.334	0.242
	$F_{abs} * \frac{f_Q Q_I CL_{ef,I}^M}{f_Q Q_I CL_{ef,I}^M + (f_Q Q_I + f_B^M CL_{in,I}^M)\left[CL_{int,met,I}^{M\to MG} + CL_{int,sec,I}^M(1-F_{abs})\right]} * \frac{(Q_I + Q_{HA})(CL_{ef,L}^M + CL_{int,sec,L}^M + CL_{int,met,L}^{M\to MG} + CL_{int,met,L}^{M\to others})}{(Q_I + Q_{HA})(CL_{ef,L}^M + CL_{int,sec,L}^M + CL_{int,met,L}^{M\to MG} + CL_{int,met,L}^{M\to others}) + f_B^M CL_{in,L}^M (CL_{int,sec,L}^M + CL_{int,met,L}^{M\to MG} + CL_{int,met,L}^{M\to others})}$	0.402	0.186
$F\{mi\}_I$	Intestinal availability of MG		
	$\frac{CL_{ef,I}^{MG}}{CL_{ef,I}^{MG} + CL_{int,sec,I}^{MG}}$	0.95	0.89
$F\{mi\}_L$	Hepatic availability of MG		
	$\frac{CL_{ef,L}^{MG}}{CL_{ef,L}^{MG} + CL_{int,sec,L}^{MG}}$	0.12	0.22
h_{mi}	Fraction of hepatic clearance of M forming MG		
	$\frac{CL_{int,met,L}^{M\to MG}}{CL_{int,met,L}^{M\to MG} + CL_{int,met,L}^{M\to others} + CL_{int,sec,L}^M}$	0.948	0.854
$g_{mi} = (1-f_e)h_{mi}$[a]	Fraction of total body clearance of M forming MG (note that f_e = 0.334 from Table 3)	0.631	0.569
$\frac{v_I}{v_I + v_L}$[b]	Fractional contribution of intestine to intestinal-liver removal	0.460 0.570[e]	0.093 0.171[e]
$\frac{v_L}{v_I + v_L}$[c]	Fractional contribution of liver to intestinal-liver removal	0.540 0.430[e]	0.907 0.829[e]

[a]Based on definition of Pang and Kwan (1983).
[b]Calculated based on equations from Pang and Chow (2012): $\frac{v_I}{v_I + v_L} = \frac{f_Q Q_I (1-F_I)}{f_Q Q_I (1-F_I) + E_L \langle Q_I [f_Q F_I + (1-f_Q)] + Q_{HA} \rangle}$
[c]Calculated based on equations from Pang and Chow (2012): $\frac{v_L}{v_I + v_L} = \frac{E_L \langle Q_I [f_Q F_I + (1-f_Q)] + Q_{HA} \rangle}{f_Q Q_I (1-F_I) + E_L \langle Q_I [f_Q F_I + (1-f_Q)] + Q_{HA} \rangle}$
[d]Equations from Pang and Sun (2010).
[e]F_I and F_L values, based on equations from Pang and Sun (2010).

Data from our study support the view that the SFM-PBPK is superior to other intestinal flow models (e.g., Q_{Gut} or TM). There has been some movement in the field to accommodate a reduced or partial intestinal flow to the enterocyte region. The emergence of the Q_{Gut} model (Yang et al., 2007) and the advanced dissolution, absorption, metabolism model from Simcyp (Darwich et al., 2010) favors this concept of partial flow. Other models that further encompass heterogeneity in transporters and enzymes have been adopted to explain the lesser intestinal metabolism observed for drugs given systemically versus orally (Tam et al., 2003; Liu et al., 2006; Bruyère et al., 2010; Gertz et al., 2010) as well as the effect of enterohepatic circulation of glucuronide conjugates (Wu, 2012). Undoubtedly, our PBPK investigation strongly supports the SFM for intestinal modeling. More importantly, the modeling approach provides essential information on the interpretation of metabolite kinetics. We are able to decipher the contributions of the intestine vs. the liver in M glucuronidation, that the intestine plays a substantial role; the opposite may be concluded for MG, which is primarily excreted by the liver. This type of PBPK modeling

TABLE 8

Discrimination between the TM-PBPK and SFM-PBPK models by the MG urine/bile ratio for intraduodenal/intravenous dosing, demonstrating the route-dependent intestinal glucuronidation of M

Model	Ratio of MG in Urine/Bile					
	Intraduodenal Dosing		Intravenous Dosing		Intraduodenal/Intravenous Dosing	
	4h	∞	4h	∞	4h	∞
Observed	0.541	^	0.212	–	2.55	—
Compartmental modeling	0.485	0.485	0.485	0.485	1.0	1.0
TM-PBPK	0.131	0.131	0.131	0.131	1.0	1.0
SFM-PBPK	0.453	0.444	0.175	0.179	2.59	2.47

^not measured.

is the first of its kind to provide detailed information on metabolite kinetics.

Appendix A: Equations for Compartmental Modeling

Rate of change of M in gut lumen for intraduodenal dosing

$$\frac{dA_G}{dt} = -k_a A_G, \quad \text{where } A_G(0) = F_{abs} \cdot \text{Dose}_{ID} \tag{1}$$

where F_{abs} is the ratio of $k_a/(k_a+k_g)$; k_a and k_g are the absorption and luminal degradation rate constants, respectively.

Rates of change of M in the central compartment

$$\frac{dC_1}{dt} = \frac{-(k_{10}+k_{12})C_1V_1 + k_aA_G + k_{21}C_2V_2}{V_1} \text{ for intraduodenal dosing} \tag{2}$$

$$\frac{dC_1}{dt} = \frac{-(k_{10}+k_{12})C_1V_1 + k_{21}C_2V_2}{V_1} \text{ for intravenous dosing} \tag{2A}$$

Rate of change of M in the peripheral compartment

$$\frac{dC_2}{dt} = \frac{-k_{21}C_2V_2 + k_{12}C_1V_1}{V_2} \tag{3}$$

Rate of change of MG or formed metabolite, denoted as {mi}

$$\frac{dC\{\text{mi}\}}{dt} = \frac{k_m C_1V_1 - k\{\text{mi}\}C\{\text{mi}\}V\{\text{mi}\}}{V\{\text{mi}\}} \tag{4}$$

Rates of biliary excretion of M and MG

$$\frac{dA_{bile}}{dt} = k_{bile}C_1V_1 \tag{5}$$

$$\frac{dA\{\text{mi}\}_{bile}}{dt} = k\{\text{mi}\}_{bile}C\{\text{mi}\}V\{\text{mi}\} \tag{6}$$

Rates of renal excretion of M and MG

$$\frac{dA_{renal}}{dt} = k_{renal}C_1V_1 \tag{7}$$

$$\frac{dA\{\text{mi}\}_{renal}}{dt} = k\{\text{mi}\}_{renal}C\{\text{mi}\}V\{\text{mi}\} \tag{8}$$

Appendix B: Equations for PBPK Modeling

Several assumptions were made: deglucuronidation of M was absent and reabsorption of MG was absent (Doherty and Pang, 2000). Once formed in the intestine or tissue, MG is effluxed out apically by Mrp2 or basolaterally by Mrp3 (van de Wetering et al., 2007) with efflux clearances $CL_{ef,I}^{MG}$ and $CL_{ef,L}^{MG}$, respectively, for the intestine and liver. MG permeates through the liver basolateral membrane with rate of 1 ml·min^{-1} (Doherty et al., 2006) but not through the intestine membrane for secretion (Doherty and Pang, 2000).

Rates of change of M and MG in the blood compartment

$$V_B\frac{dM_B}{dt} = Q_{RP}\frac{M_{RP}}{K_{RP}} + Q_{PP}\frac{M_{PP}}{K_{PP}} + Q_{AD}\frac{M_{AD}}{K_{AD}} + (Q_I + Q_{HA})M_{LB} - (Q_I + Q_{HA} + Q_{RP} + Q_{PP} + Q_{AD})M_B - f_B M_B CL_R^M \tag{9}$$

$$V_B\frac{dMG_B}{dt} = (Q_I + Q_{HA})(MG_{LB} - MG_B) - f_B MG_B CL_R^{MG} \tag{10}$$

Rate of change of M in rapidly perfused tissue

$$V_{RP}\frac{dM_{RP}}{dt} = Q_{RP}M_B - Q_{RP}\frac{M_{RP}}{K_{RP}} \tag{11}$$

Rate of change of M in poorly perfused tissue

$$V_{PP}\frac{dM_{PP}}{dt} = Q_{PP}M_B - Q_{PP}\frac{M_{PP}}{K_{PP}} \tag{12}$$

Rate of change of M in adipose tissue

$$V_{AD}\frac{dM_{AD}}{dt} = Q_{AD}M_B - Q_{AD}\frac{M_{AD}}{K_{AD}} \tag{13}$$

For the Intestine and Liver according to the TM

Rates of change of M and MG in the intestine, I

$$V_I\frac{dM_I}{dt} = f_B^M M_{IB}CL_{in,I}^M - f_I^M M_I(CL_{int,met,I}^{M\to MG} + CL_{int,sec,I}^M + CL_{ef,I}^M) + k_a A_{lumen}^M \tag{14}$$

$$V_I\frac{dMG_I}{dt} = f_I^M M_I CL_{int,met,I}^{M\to MG} - f_I^{MG} MG_I(CL_{int,sec,I}^{MG} + CL_{ef,I}^{MG}) \tag{15}$$

Rates of change of M and MG in intestinal blood, IB

$$V_{IB}\frac{dM_{IB}}{dt} = Q_I(M_B - M_{IB}) - f_B^M M_{IB}CL_{In,I}^M + f_I^M M_I CL_{ef,I}^M \tag{16}$$

$$V_{IB}\frac{dMG_{IB}}{dt} = Q_I(MG_B - MG_{IB}) + f_I^{MG} MG_I CL_{ef,I}^{MG} \tag{17}$$

Rates of change of M and MG in the liver, L

$$V_L\frac{dM_L}{dt} = f_B^M M_{LB} CL_{in,L}^M - f_L^M M_L (CL_{int,met,L}^{M\rightarrow MG} + CL_{int,met,L}^{M\rightarrow Others} + CL_{int,sec,L}^M + CL_{ef,L}^M) \quad (18)$$

$$V_L\frac{dMG_L}{dt} = f_L^M M_L CL_{int,met,L}^{M\rightarrow MG} - f_L^{MG} MG_L (CL_{int,sec,L}^{MG} + CL_{ef,L}^{MG}) + f_B^{MG} MG_{LB} CL_{in,L}^{MG} \quad (19)$$

Rates of change of M and MG in liver blood, LB

$$V_{LB}\frac{dM_{LB}}{dt} = Q_{HA}M_B + Q_I M_{IB} - (Q_{HA}+Q_I)M_{LB} + f_L^M M_L CL_{ef,L}^M - f_B^M M_{LB} CL_{in,L}^M \quad (20)$$

$$V_{LB}\frac{dMG_{LB}}{dt} = Q_{HA}MG_B + Q_I MG_{IB} - (Q_{HA}+Q_I)MG_{LB} + f_L^{MG} MG_L CL_{ef,L}^{MG} - f_B^{MG} MG_{LB} CL_{in,L}^{MG} \quad (21)$$

For the Intestine and Liver according to the SFM

Rates of change of M and MG in the enterocyte, en

$$V_{en}\frac{dM_{en}}{dt} = f_B^M M_{enb} CL_{in,I}^M - f_I^M M_{en}\left(CL_{int,met,I}^{M\rightarrow MG} + CL_{int,sec,I}^M + CL_{ef,I}^M\right) + k_a A_{lumen}^M \quad (22)$$

$$V_{en}\frac{dMG_{en}}{dt} = f_I^M M_{en} CL_{int,met,I}^{M\rightarrow MG} - f_I^{MG} MG_{en}\left(CL_{ef,I}^{MG} + CL_{int,sec,I}^{MG}\right) \quad (23)$$

Rates of change of M and MG in enterocyte blood, enB

$$V_{enB}\frac{dM_{enB}}{dt} = f_Q Q_I (M_B - M_{enB}) + f_I^M M_{en} CL_{ef,I}^M - f_B^M M_{enB} CL_{In,I}^M \quad (24)$$

$$V_{enB}\frac{dMG_{enB}}{dt} = f_Q Q_I (MG_B - MG_{enB}) + f_I^{MG} MG_{en} CL_{ef,I}^{MG} \quad (25)$$

Rates of change of M and MG in serosa, s

$$V_s\frac{dM_s}{dt} = f_B^M M_{sB} CL_{in,I}^M - f_I^M M_s CL_{ef,I}^M$$
$$V_s\frac{dMG_s}{dt} = 0 \quad (26)$$

Rates of change of M and MG in serosal blood, sB

$$V_{sB}\frac{dM_{sB}}{dt} = (1-f_Q)Q_I(M_B - M_{sB}) + f_I^M M_s CL_{ef,I}^M - f_B^M M_{sB} CL_{In,I}^M$$
$$V_{sB}\frac{dMG_{sB}}{dt} = 0 \quad (27)$$

Rates of change of M and MG in liver blood, LB

$$V_{LB}\frac{dM_{LB}}{dt} = Q_{HA}M_B + f_Q Q_I M_{enB} + (1-f_Q)Q_I M_{sB} - (Q_{HA}+Q_I)M_{LB} + f_L^M M_L CL_{ef,L}^M - f_B^M M_{LB} CL_{in,L}^M \quad (28)$$

$$V_{LB}\frac{dMG_{LB}}{dt} = Q_{HA}MG_B + f_Q Q_I MG_{enB} + (1-f_Q)Q_I MG_{sB} - (Q_{HA}+Q_I)MG_{LB} + f_L^{MG} MG_L CL_{ef,L}^{MG} - f_B^{MG} MG_{LB} CL_{in,L}^{MG} \quad (29)$$

Rates of change of M and MG in the liver, L: same equations (equations 18 and 19) as for the TM

Rates of change of M and MG in the gut lumen

$$\frac{dA_{lumen}^M}{dt} = -k_a A_{lumen}^M + f_I^M M_I CL_{int,sec,I}(\text{TM}) \quad or \quad -k_a A_{lumen}^M + f_I^M M_{en} CL_{int,sec,I}(\text{SFM}) \quad (30)$$

$$\frac{dA_{lumen}^{MG}}{dt} = f_I^{MG} MG_I CL_{int,sec,I}^{MG}(\text{ for TM}) \quad or \quad f_I^{MG} MG_{en} CL_{int,sec,I}^{MG}(\text{ for SFM}) \quad (31)$$

Rates of change of M and MG in bile for both the TM and SFM

$$\frac{dA_{bile}^M}{dt} = f_L^M M_L CL_{int,sec,L} \quad (32)$$

$$\frac{dA_{bile}^{MG}}{dt} = f_L^{MG} MG_L CL_{int,sec,L}^{MG} \quad (33)$$

Rates of change of M and MG in urine for both TM and SFM

$$\frac{dA_{urine}^M}{dt} = f_B^M M_B CL_R^M \quad (34)$$

$$\frac{dA_{urine}^{MG}}{dt} = f_B^{MG} MG_B CL_R^{MG} \quad (35)$$

Acknowledgments

The authors thank Dr. Carolyn Cummins (Leslie Dan Faculty of Pharmacy, University of Toronto, Toronto, ON, Canada) for use of her LC-MS equipment.

Authorship Contributions

Participated in research design: Fan, Chen, Pang.
Conducted experiments: Fan, Chen, Sun.
Performed data analysis: Yang, Fan, Chen, Liu, Sun, Pang.
Wrote or contributed to the writing of the manuscript: Yang, Fan, Chen, Pang.

References

Böerner U (1975) The metabolism of morphine and heroin in man. *Drug Metab Rev* **4**:39–73.
Boxenbaum HG, Riegelman S, and Elashoff RM (1974) Statistical estimations in pharmacokinetics. *J Pharmacokinet Biopharm* **2**:123–148.
Bruyère A, Declèves X, Bouzom F, Ball K, Marques C, Treton X, Pocard M, Valleur P, Bouhnik Y, and Panis Y, et al. (2010) Effect of variations in the amounts of P-glycoprotein (ABCB1), BCRP (ABCG2) and CYP3A4 along the human small intestine on PBPK models for predicting intestinal first pass. *Mol Pharm* **7**:1596–1607.
Cassidy MK and Houston JB (1984) In vivo capacity of hepatic and extrahepatic enzymes to conjugate phenol. *Drug Metab Dispos* **12**:619–624.
Chow EC and Pang KS (2013) Why we need proper PBPK models to examine intestine and liver oral drug absorption. *Curr Drug Metab* **14**:57–79.
Cong D, Doherty M, and Pang KS (2000) A new physiologically based, segregated-flow model to explain route-dependent intestinal metabolism. *Drug Metab Dispos* **28**:224–235.
Corley RA, Bartels MJ, Carney EW, Weitz KK, Soelberg JJ, Gies RA, and Thrall KD (2005) Development of a physiologically based pharmacokinetic model for ethylene glycol and its metabolite, glycolic acid, in rats and humans. *Toxicol Sci* **85**:476–490.
Dahlström BE and Paalzow LK (1978) Pharmacokinetic interpretation of the enterohepatic recirculation and first-pass elimination of morphine in the rat. *J Pharmacokinet Biopharm* **6**: 505–519.
Darwich AS, Neuhoff S, Jamei M, and Rostami-Hodjegan A (2010) Interplay of metabolism and transport in determining oral drug absorption and gut wall metabolism: a simulation assessment using the "Advanced Dissolution, Absorption, Metabolism (ADAM)" model. *Curr Drug Metab* **11**:716–729.
Davies B and Morris T (1993) Physiological parameters in laboratory animals and humans. *Pharm Res* **10**:1093–1095.
de Lannoy IA and Pang KS (1986) Presence of a diffusional barrier on metabolite kinetics: enalaprilat as a generated versus preformed metabolite. *Drug Metab Dispos* **14**:513–520.

de Lannoy IA and Pang KS (1993) Combined recirculation of the rat liver and kidney: studies with enalapril and enalaprilat. *J Pharmacokinet Biopharm* **21**:423–456.
Doherty MM and Pang KS (2000) Route-dependent metabolism of morphine in the vascularly perfused rat small intestine preparation. *Pharm Res* **17**:291–298.
Doherty MM, Poon K, Tsang C, and Pang KS (2006) Transport is not rate-limiting in morphine glucuronidation in the single-pass perfused rat liver preparation. *J Pharmacol Exp Ther* **317**: 890–900.
Everett NB, Simmons B, and Lasher EP (1956) Distribution of blood (Fe 59) and plasma (I 131) volumes of rats determined by liquid nitrogen freezing. *Circ Res* **4**:419–424.
Fan J, Chen S, Chow EC, and Pang KS (2010) PBPK modeling of intestinal and liver enzymes and transporters in drug absorption and sequential metabolism. *Curr Drug Metab* **11**:743–761.
Gao G and Law FC (2009) Physiologically based pharmacokinetics of matrine in the rat after oral administration of pure chemical and ACAPHA. *Drug Metab Dispos* **37**:884–891.
Gertz M, Harrison A, Houston JB, and Galetin A (2010) Prediction of human intestinal first-pass metabolism of 25 CYP3A substrates from in vitro clearance and permeability data. *Drug Metab Dispos* **38**:1147–1158.
Giacomini KM, Nakeeb SM, and Levy G (1980) Pharmacokinetic studies of propoxyphene I: effect of portacaval shunt on systemic availability in dogs. *J Pharm Sci* **69**:786–789.
Gugler R, Lain P, and Azarnoff DL (1975) Effect of portacaval shunt on the disposition of drugs with and without first-pass effect. *J Pharmacol Exp Ther* **195**:416–423.
Hirayama H, Morgado J, Gasinska I, and Pang KS (1990) Estimations of intestinal and liver first-pass metabolism in vivo. Studies on gentisamide conjugation in the rat. *Drug Metab Dispos* **18**: 588–594.
Horton TL and Pollack GM (1991) Enterohepatic recirculation and renal metabolism of morphine in the rat. *J Pharm Sci* **80**:1147–1152.
Iwamoto K and Klaassen CD (1977) First-pass effect of morphine in rats. *J Pharmacol Exp Ther* **200**:236–244.
Iwamoto K, Takei M, and Watanabe J (1982) Gastrointestinal and hepatic first-pass metabolism of aspirin in rats. *J Pharm Pharmacol* **34**:176–180.
Letrent SP, Polli JW, Humphreys JE, Pollack GM, Brouwer KR, and Brouwer KL (1999) P-Glycoprotein-mediated transport of morphine in brain capillary endothelial cells. *Biochem Pharmacol* **58**:951–957.
Liu S, Tam D, Chen X, and Pang KS (2006) P-glycoprotein and an unstirred water layer barring digoxin absorption in the vascularly perfused rat small intestine preparation: induction studies with pregnenolone-16α-carbonitrile. *Drug Metab Dispos* **34**:1468–1479.
Liu YT, Hao HP, Xie HG, Lai L, Wang Q, Liu CX, and Wang GJ (2010) Extensive intestinal first-pass elimination and predominant hepatic distribution of berberine explain its low plasma levels in rats. *Drug Metab Dispos* **38**:1779–1784.
Lown KS, Thummel KE, Benedict PE, Shen DD, Turgeon DK, Berent S, and Watkins PB (1995) The erythromycin breath test predicts the clearance of midazolam. *Clin Pharmacol Ther* **57**: 16–24.
Marcel de Vries PA, Navis G, de Boer E, de Jong PE, and de Zeeuw D (1997) A method for accurate measurement of GFR in conscious, spontaneously voiding rats. *Kidney Int* **52**:244–247.
Mistry M and Houston JB (1987) Glucuronidation in vitro and in vivo. Comparison of intestinal and hepatic conjugation of morphine, naloxone, and buprenorphine. *Drug Metab Dispos* **15**: 710–717.
Paine MF, Shen DD, Kunze KL, Perkins JD, Marsh CL, McVicar JP, Barr DM, Gillies BS, and Thummel KE (1996) First-pass metabolism of midazolam by the human intestine. *Clin Pharmacol Ther* **60**:14–24.
Pang KS (2003) Modeling of intestinal drug absorption: roles of transporters and metabolic enzymes (for the Gillette Review Series). *Drug Metab Dispos* **31**:1507–1519.
Pang KS (2009) Safety testing of metabolites: expectations and outcomes. *Chem Biol Interact* **179**: 45–59.
Pang KS, Cherry WF, and Ulm EH (1985) Disposition of enalapril in the perfused rat intestine-liver preparation: absorption, metabolism and first-pass effect. *J Pharmacol Exp Ther* **233**:788–795.
Pang KS and Chow EC (2012) Commentary: theoretical predictions of flow effects on intestinal and systemic availability in physiologically based pharmacokinetic intestine models: the traditional model, segregated flow model, and QGut model. *Drug Metab Dispos* **40**:1869–1877.
Pang KS and Gillette JR (1979) Sequential first-pass elimination of a metabolite derived from a precursor. *J Pharmacokinet Biopharm* **7**:275–290.
Pang KS and Kwan KC (1983) A commentary: methods and assumptions in the kinetic estimation of metabolite formation. *Drug Metab Dispos* **11**:79–84.
Pang KS, Maeng HJ, and Fan J (2009) Interplay of transporters and enzymes in drug and metabolite processing. *Mol Pharm* **6**:1734–1755.
Pang KS, Morris ME, and Sun H (2008) Formed and preformed metabolites: facts and comparisons. *J Pharm Pharmacol* **60**:1247–1275.
Peters SA (2008) Evaluation of a generic physiologically based pharmacokinetic model for lineshape analysis. *Clin Pharmacokinet* **47**:261–275.
Plänitz V, Grönniger J, and Jähnchen E (1985) Prehepatic and hepatic first-pass metabolism of lorcainide in rats. *Arzneimittelforschung* **35**:923–926.
Projean D, Morin PE, Tu TM, and Ducharme J (2003) Identification of CYP3A4 and CYP2C8 as the major cytochrome P450s responsible for morphine N-demethylation in human liver microsomes. *Xenobiotica* **33**:841–854.
Qi X, Evans AM, Wang J, Miners JO, Upton RN, and Milne RW (2010) Inhibition of morphine metabolism by ketamine. *Drug Metab Dispos* **38**:728–731.
Rane A, Gawronska-Szklarz B, and Svensson JO (1985) Natural (-)- and unnatural (+)-enantiomers of morphine: comparative metabolism and effect of morphine and phenobarbital treatment. *J Pharmacol Exp Ther* **234**:761–765.
Rodgers T and Rowland M (2006) Physiologically based pharmacokinetic modelling 2: predicting the tissue distribution of acids, very weak bases, neutrals and zwitterions. *J Pharm Sci* **95**:1238–1257.
Rodgers T and Rowland M (2007) Mechanistic approaches to volume of distribution predictions: understanding the processes. *Pharm Res* **24**:918–933.
Shanahan KM, Evans AM, and Nation RL (1997) Disposition of morphine in the rat isolated perfused kidney: concentration ranging studies. *J Pharmacol Exp Ther* **282**:1518–1525.
Sun H, Liu L, and Pang KS (2006) Increased estrogen sulfation of estradiol 17β-D-glucuronide in metastatic tumor rat livers. *J Pharmacol Exp Ther* **319**:818–831.
Sun H and Pang KS (2010) Physiological modeling to understand the impact of enzymes and transporters on drug and metabolite data and bioavailability estimates. *Pharm Res* **27**:1237–1254.
Sun H, Zeng YY, and Pang KS (2010) Interplay of phase II enzymes and transporters in futile cycling: influence of multidrug resistance-associated protein 2-mediated excretion of estradiol 17β-D-glucuronide and its 3-sulfate metabolite on net sulfation in perfused TR(−) and Wistar rat liver preparations. *Drug Metab Dispos* **38**:769–780.
Tam D, Tirona RG, and Pang KS (2003) Segmental intestinal transporters and metabolic enzymes on intestinal drug absorption. *Drug Metab Dispos* **31**:373–383.
Van Crugten JT, Sallustio BC, Nation RL, and Somogyi AA (1991) Renal tubular transport of morphine, morphine-6-glucuronide, and morphine-3-glucuronide in the isolated perfused rat kidney. *Drug Metab Dispos* **19**:1087–1092.
van de Wetering K, Zelcer N, Kuil A, Feddema W, Hillebrand M, Vlaming ML, Schinkel AH, Beijnen JH, and Borst P (2007) Multidrug resistance proteins 2 and 3 provide alternative routes for hepatic excretion of morphine-glucuronides. *Mol Pharmacol* **72**:387–394.
van Herwaarden AE, Wagenaar E, van der Kruijssen CM, van Waterschoot RA, Smit JW, Song JY, van der Valk MA, van Tellingen O, van der Hoorn JW, and Rosing H, et al. (2007) Knockout of cytochrome P450 3A yields new mouse models for understanding xenobiotic metabolism. *J Clin Invest* **117**:3583–3592.
Wandel C, Kim R, Wood M, and Wood A (2002) Interaction of morphine, fentanyl, sufentanil, alfentanil, and loperamide with the efflux drug transporter P-glycoprotein. *Anesthesiology* **96**: 913–920.
Wu B (2012) Use of physiologically based pharmacokinetic models to evaluate the impact of intestinal glucuronide hydrolysis on the pharmacokinetics of aglycone. *J Pharm Sci* **101**: 1281–1301.
Yang J, Jamei M, Yeo KR, Tucker GT, and Rostami-Hodjegan A (2007) Prediction of intestinal first-pass drug metabolism. *Curr Drug Metab* **8**:676–684.
Zhang QY, Fang C, Zhang J, Dunbar D, Kaminsky L, and Ding X (2009) An intestinal epithelium-specific cytochrome P450 (P450) reductase-knockout mouse model: direct evidence for a role of intestinal p450s in first-pass clearance of oral nifedipine. *Drug Metab Dispos* **37**:651–657.
Zhang QY, Kaminsky LS, Dunbar D, Zhang J, and Ding X (2007) Role of small intestinal cytochromes p450 in the bioavailability of oral nifedipine. *Drug Metab Dispos* **35**:1617–1623.

Address correspondence to: Dr. K. Sandy Pang, Leslie Dan Faculty of Pharmacy, University of Toronto, 144 College Street, Toronto, ON M5S 3M2, Canada. E-mail: ks.pang@utoronto.ca